

Liquid desiccant dehumidification and regeneration process: Advancing correlations for moisture and enthalpy effectiveness

Alessandro Giampieri^{*}, Zhiwei Ma, Janie Ling-Chin, Huashan Bao, Andrew J. Smallbone, Anthony Paul Roskilly

Department of Engineering, Durham University, Durham DH1 3LE, United Kingdom

HIGHLIGHTS

- Focused on the liquid desiccant dehumidification and regeneration process.
- Correlations for predicting moisture and enthalpy effectiveness were developed.
- System dimensions, solutions and packing materials/structures were considered.
- Useful for quick design and analysis to establish cost-effective solutions.

ARTICLE INFO

Keywords:

Liquid desiccant
Dehumidification
Regeneration
Moisture and enthalpy effectiveness
Correlation development
Regression analysis

ABSTRACT

The paper developed correlations for predicting moisture and enthalpy effectiveness of the liquid desiccant dehumidification and regeneration process. Experimental dehumidification and regeneration data available from the literature with different system dimensions, liquid desiccant solutions (LiBr and LiCl), geometry and size of the packing and flow configuration (counter- and cross-flow) were gathered for correlations development. The developed correlations involved the mass flow rates of air and desiccant solution, the inlet temperature of the air and the desiccant solution, the moisture content and enthalpy of the inlet air, the moisture content and enthalpy of air at an equilibrium state with the inlet desiccant solution, the geometry, dimensions and wetting of the packing and the contact time between air and desiccant solution. The comparison between the calculated and experimental effectiveness showed a good match, which had errors ranging 4.37–7.2%, and performed better when compared to other correlations available in the literature. These newly developed correlations will be useful for quick system design and performance analysis and to establish cost-effective solutions for liquid desiccant technology.

1. Introduction

Liquid desiccant technology has been identified as one of the most promising energy-efficient and environmentally-friendly technologies for temperature and humidity control in a wide range of applications [1,2], including moisture control and removal, production of dry air for evaporative cooling, assistance of low-temperature drying [3] and decoupling of sensible and latent heat in combination with a heat pump [4]. Coupled and complicated heat and mass transfer exists in the dehumidification and regeneration process of the liquid desiccant technology: the difference between the temperature of the air, T_a , and that of the desiccant solution, T_{sol} , and the difference between the

vapour pressure of the air, which is related to the moisture content, ω_a , and the equilibrium vapour pressure of the desiccant solution, which is related to the equilibrium moisture content, $\omega_{eq,sol}$, are the driving forces for heat and mass transfer, respectively; the heat transfer changes the solution temperature and its equilibrium vapour pressure, affecting the mass transfer potential that changes with the varying vapour pressure difference. A graphical illustration of the relationship is shown in Fig. 1 [5].

Theoretical analysis, experimental modelling and soft computing techniques are among the modelling strategies used to investigate the coupled heat and mass transfer between air and solution and to predict the performance of liquid desiccant systems [6]. The theoretical analysis entails using mathematical models to evaluate the performance of the

^{*} Corresponding author.

E-mail address: alessandro.giampieri@durham.ac.uk (A. Giampieri).

Nomenclature			
A	cross-section area (m^2)	y	corrugation height of structured packing (m)
a_e	effective area to volume ratio (m^2/m^3)	Z	height of the packing material (m)
a_p	surface area to volume ratio (m^2/m^3)	<i>Greeks</i>	
a_w	wetted area to volume ratio (m^2/m^3)	ε	effectiveness (-)
b	corrugation base length of structured packing (m)	θ	corrugation angle ($^\circ$)
C	constants in the correlation	μ	dynamic viscosity (Pa·s)
d_{eq}	equivalent diameter of the packing (m)	ρ	density (kg/m^3)
e	void ratio of structured packing (-)	σ	surface tension (N/m)
H	hold-up (m^3/m^3)	ω	moisture content ($kg_{H_2O}/kg_{dry,air}$)
h	enthalpy (kJ/kg)	<i>Subscripts</i>	
L	length of the packing material (m)	a	air
m	mass flow rate (kg/s)	da	dry air
P	pressure (Pa)	dy	dynamic
q	volumetric flow rate ($m^3/(m^2 \cdot h)$)	eq, sol	equilibrium solution
S	superficial mass flow rate ($kg/(m^2 \cdot s)$)	in	inlet
s	corrugation side length of structured packing (m)	K	Kelvin
T	temperature ($^\circ C$)	m	moisture
t	air-desiccant contact time (s)	out	outlet
U	superficial velocity (m/s)	sol	solution
W	width of the packing material (m)	st	static
x	liquid desiccant solution mass fraction ($kg_{desiccant}/kg_{solution}$)	w	water

dehumidifier/regenerator via stepwise heat and mass balance across the packed bed with transfer coefficients calculated at each step [7]. Several studies [7–11] have focused on determining these coefficients for packed columns in liquid desiccant systems based on operational parameters such as air/desiccant contact surface and flow configuration (counter, cross, or parallel flow), as well as thermodynamic and transport parameters of both ambient air and desiccant solution. Detailed mathematical models have been developed to express the coupled heat and mass transfer process [12,13], such as finite difference [14–16], effectiveness-number of transfer units (ε -NTU) [17–19] and simplified models [20,21]. Because of the complex interfacial transfer process, these theoretical models should be validated against experimental results where the analysis and performance prediction are complex and at a very high computational cost. The finite difference and ε -NTU model are too complicated to be used for a yearly hour-by-hour performance analysis [13]. Experimental modelling is time and cost consuming, requiring long experiments with expensive laboratory equipment and

reliable instrumentation [22] and difficulties in validating numerical and analytical models using experimental results were found in the literature [23].

Unlike experimental modelling, predictive models based on correlations (for example, moisture and enthalpy effectiveness correlations) can be quickly used for performance analysis and design of liquid desiccant systems. Various correlations have been developed for the study of the effectiveness parameters of these systems based on experimental and theoretical analysis [24]. Table 1 summarises correlations of moisture and enthalpy effectiveness available in the literature for the dehumidification and regeneration process, including the variables involved, the conditions under which the correlations were developed (packing material structure and flow configuration) and the limitations. The complete equations of the correlations for the dehumidification and regeneration process are presented in Appendix A.

All correlations were validated against experimental results obtained from primary or secondary sources, such as experiments or literature.

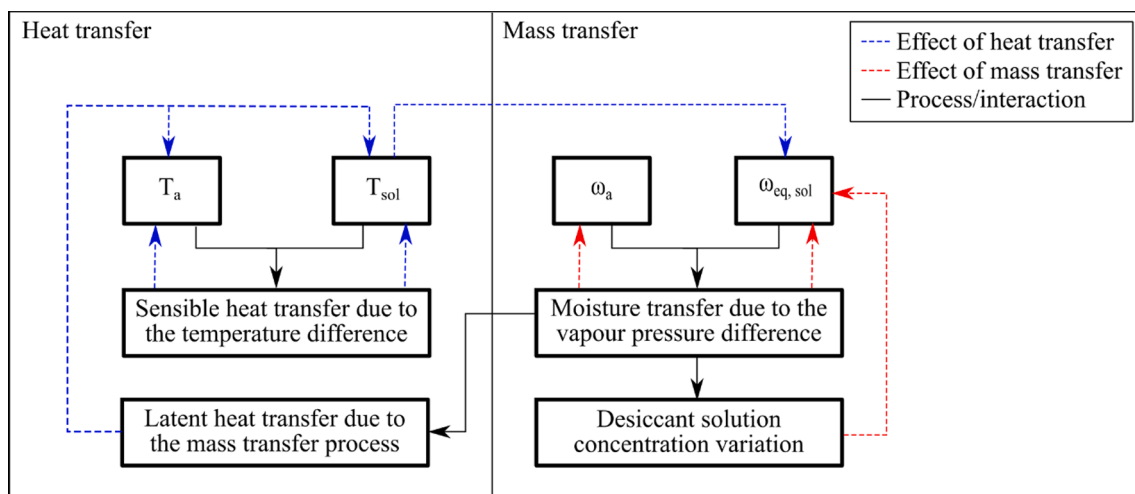


Fig. 1. Coupled heat and mass transfer between air and liquid desiccant, adapted from [5].

Table 1
Correlations for predicting moisture and enthalpy effectiveness in the dehumidification and regeneration process.

	Ref.	Parameters	Packing structure	Flow	Methodology of development and accuracy	Limitation
Dehumidification	[25]	$\epsilon_w = f(m_a, m_{sol}, T_a, T_{sol}, P_{sol}, P_w, a_p Z)$	Random	Counter-flow	Validated by own experiments. 93% of the calculation error was lower than $\pm 10\%$.	Ambient humidity was not assessed. Limited to its specific packing and flow configuration.
	[26]	$\epsilon_w = f(m_a, m_{sol}, T_a, T_{sol}, P_{sol}, P_w, a_p Z)$	Random	Counter-flow	Validated by own and other experimental data. 80% of data points showed error lower than $\pm 10\%$ with average value of about 9.96%.	Ambient humidity was not assessed. Limited to its specific packing and flow configuration.
	[27]	$\epsilon_w, \epsilon_h = f(S_a, S_{sol}, h_a, h_{eq, sol}, \sigma_{sol}, \sigma_c, a_p Z)$	Random	Counter-flow	Validated by experimental results from four publications. Errors lower than $\pm 15\%$. Wetting characteristics of the desiccant solution and packing as two of the variables (σ_{sol} and σ_c)	Uncoupled effect of sensible and latent heat transfer not assessed. Limited to its specific flow configuration.
	[28]	$\epsilon_w = f(m_{sol}, T_a, a_p)$	Structured	Counter-flow	Correlation obtained through stepwise regression from own experimental data. Errors from 6 experimental data lower than $\pm 20\%$.	Ambient humidity and air flow rate were not assessed. Geometry of the packing was not considered.
	[20]	$\epsilon_w = f(m_a, m_{sol}) \epsilon_h = f(m_a, m_{sol}, h_a, h_{eq, sol}, \omega_a, \omega_{eq, sol})$	Structured	Cross-flow	Correlation regressed from own experimental data. Errors of 6.3% and 6% for the moisture and enthalpy effectiveness. Reported good agreement with data in the literature.	Temperature and moisture content were not assessed in the correlation for ϵ_w . Packing material not assessed.
	[29]	$\epsilon_w = f(S_a, S_{sol}, T_a, T_{sol}, x_{sol})$	Structured	Cross-flow	Developed by data fitting from 179 experimental runs with the correlations proposed by Ullah <i>et al.</i> [6] and Chung [25]. 99.4% of the calculations showed errors lower than $\pm 20\%$.	Ambient humidity and packing material were not assessed. Applicable only to LiBr solution.
	[30]	$\epsilon_w = f(m_a, m_{sol}, T_a, T_{sol}, P_{sol}, P_w)$	Structured	Cross-flow	Correlation from own experimental data of a cross flow dehumidifier, which showed errors lower than $\pm 10\%$.	Ambient humidity and packing material were not assessed.
	[31]	$\epsilon_w = f(m_a, m_{sol}, T_a, T_{sol}, \omega_a, x_{sol}) \epsilon_h = f(m_a, m_{sol}, h_a, h_{eq, sol}, \omega_a, \omega_{eq, sol})$	Structured	Cross-flow	Correlation regressed from 88 and 54 experimental data for LiBr and LiCl desiccant solution with an average error of 9.1% and 7%, respectively.	Different equations for LiBr and LiCl solution. Applicable only to specific desiccant. Packing material was not assessed.
	[32]	$\epsilon_w = f(m_a, m_{sol}) \epsilon_h = f(m_a, m_{sol}, h_a, h_{eq, sol}, \omega_a, \omega_{eq, sol})$	Structured	Cross-flow	Correlation obtained through stepwise regression based on 48 sets of experimental results. 91.2% of the calculation had the error less than $\pm 10\%$.	Packing material was not assessed. Moisture removal ability was not considered in the correlation for ϵ_w .
	[33]	$\epsilon_w = f(m_a, m_{sol}, T_a, T_{sol}, \omega_a) \epsilon_h = f(m_a, m_{sol}, T_a, T_{sol}, \omega_a)$	Structured	Counter-flow	Stepwise regression from own experimental data. Errors of 5.16% and 5% for the moisture and enthalpy effectiveness. Validated using experimental data from [34].	Packing material and moisture removal ability of the desiccant solution were not assessed.
Regeneration	[27]	$\epsilon_w, \epsilon_h = f(S_a, S_{sol}, h_a, h_{eq, sol}, \sigma_{sol}, \sigma_c, a_p Z)$	Random	Counter-flow	Validated by experimental results from four publications. Errors lower than $\pm 15\%$. Wetting characteristics of the desiccant solution and packing as two of the variables (σ_{sol} and σ_c).	Uncoupled effect of sensible and latent heat transfer was not assessed. Limited to its specific flow configuration.
	[35]	$\epsilon_w = f(m_a, T_a, \omega_a, T_{sol}, x_{sol}, \omega_{eq, sol})$	Structured	Counter-flow	Correlation regressed from 86 experimental runs. 95.3% of the calculation had the error less than $\pm 30\%$.	Solution flow rate and packing material was not assessed.
	[36]	$\epsilon_w = f(m_a, m_{sol}, \omega_a, T_{sol}, x_{sol})$	Structured	Cross-flow	Correlation obtained through stepwise regression, around 96% of the 73 sets of runs were within the error of $\pm 10\%$.	Air temperature and packing material was not assessed. Applicable only to LiBr solution.
	[31]	$\epsilon_w = f(m_a, m_{sol}, T_a, T_{sol}, \omega_a, x_{sol}) \epsilon_h = f(m_a, m_{sol}, h_a, h_{eq, sol}, \omega_a, \omega_{eq, sol})$	Structured	Cross-flow	Correlation regressed from 82 and 56 experimental data for LiBr and LiCl desiccant solution with an average error of 3.8% and 7.5%, respectively.	Different equations for LiBr and LiCl solution. Applicable only to specific desiccant. Packing material was not assessed.

Table 1 shows the knowledge gap of current correlations for dehumidification and regeneration process analysis: these correlations are unsatisfactory in terms of application range and accuracy (as they are limited to a specific type of packing material, liquid desiccant solution or flow pattern) and produce large errors when applied to systems other than those used for validation. Furthermore, despite the fact that it is equally important in reflecting the combined heat and mass transfer of the liquid desiccant process, the enthalpy effectiveness correlation is rarely reported. In addition, numerous moisture effectiveness correlations have been proposed in the literature for various desiccant solutions and dehumidifier structures, but little is published for the regenerator.

To overcome the limits and gaps of correlations currently available in the literature, novel correlations for the moisture and enthalpy

effectiveness of both the dehumidification and regeneration process were developed. The novelty and originality of this study is justified as follows:

- Whilst collecting primary data is expensive, this study is the first to use only secondary data (*i.e.* experimental data available in the literature) and consider parameters previously neglected, such as contact time, hold-up-based wetting and effective interfacial area, in developing new correlations for the dehumidification and regeneration process of liquid desiccants.
- Based on theoretical analysis of previous correlations and identification of the main parameters affecting the coupled heat and mass transfer process between air and desiccant solution, this study offers

new correlations developed for the regeneration process along with dehumidification, which advances existing knowledge and resolves the issue of the lack of correlations for the regeneration process.

In comparison to existing correlations, the newly developed ones aim to be applicable to different flow rates, desiccant solutions (characterised by their thermodynamic functions), flow configuration and packing geometry and size. These new correlations will enable (1) quick performance prediction of liquid desiccant technology on a yearly hour-by-hour basis for various applications and (2) easy estimation of the capital (e.g. system and liquid desiccant solutions) and operating (e.g. solution pumping, air blowing, cooling towers, etc.) costs, which would assist in the determination of energy- and cost-effective measures and the realisation of techno-economic optimisation analysis for the technology. The correlations can be used to evaluate the performance of the coupled heat and mass transfer process for both dehumidification and regeneration, which is especially useful in applications where the technology is used not only for moisture control but also for heat recovery, heating and cooling. In addition, they could aid with the design of thermo-chemical district networks [37,38] by enabling rapid control of the regeneration process and quick estimation of the required air and solution flow rates in line with the variation in temperature of the

available heat source (industrial heat, combined heat and power, solar energy, etc.) and the outdoor air condition.

The paper is structured as follows. After a brief description of the liquid desiccant technology and the parameters used for its performance evaluation in Section 2, Section 3 describes the applicable scope of the research and the methodology used for the development of the correlations, which is performed in Section 4, based on analysis of existing correlations, parameters selection, data collection from experiments and statistical analysis. The discussion is supported in Section 5 by the estimation of the accuracy of newly developed correlations and the comparison with correlations available in the literature.

2. Working principle and definition

Liquid desiccants are solutions with hygroscopic properties characterised by a high affinity for water vapour molecules. Desiccant solutions include metal halide salt solutions (such as LiCl, LiBr, and CaCl₂), salts of weak organic acids (such as HCO₂K), try-ethylene glycol (TEG) and ionic liquids [39]. A typical liquid desiccant system consists of a dehumidifier (also known as an absorber), a regenerator (also known as a desorber), heat exchangers (at the heat source, heat sink and solution-to-solution; one each), fans (to blow air) and pumps (to circulate the

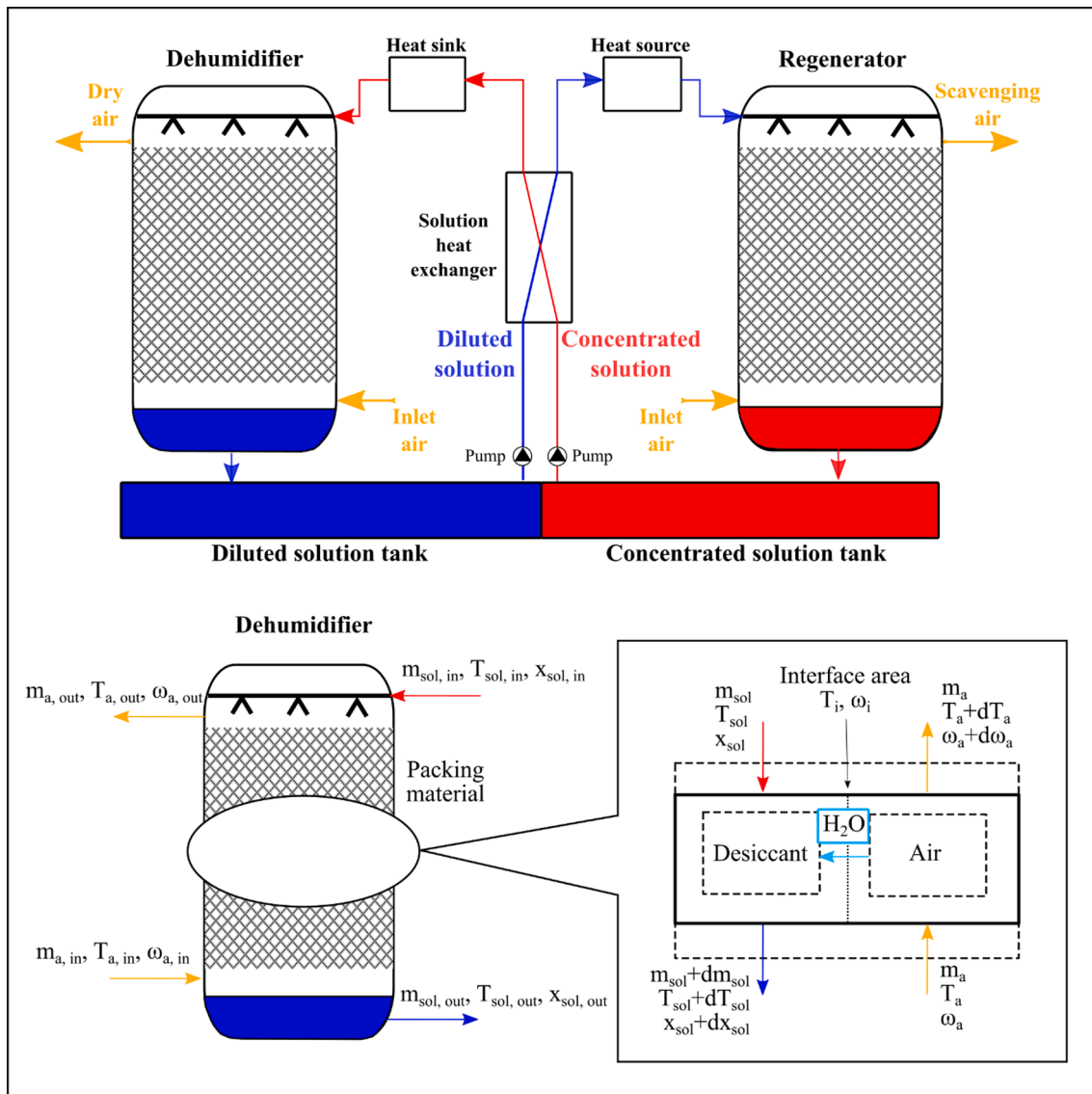


Fig. 2. Liquid desiccant system and heat and mass transfer in a counter-flow dehumidifier packed column.

desiccant solution). The regenerator and dehumidifier are both containers with nozzles on the top that spray diluted and concentrated liquid desiccant solutions, respectively. Typically, these containers are filled with packing material to provide a contact surface and improve heat and mass transfer between the air and the solution.

Fig. 2 depicts the liquid desiccant system, along with the dehumidifier packed tower and its coupled heat and mass transfer process. The desiccant solution in the dehumidifier has a low equilibrium vapour pressure to allow for moisture removal from the air, which dilutes the solution and releases heat of absorption. This exothermic process is driven by the difference between the air vapour pressure and the equilibrium vapour pressure of the concentrated liquid desiccant solution. The capacity of the concentrated desiccant solution to absorb moisture is proportional to its concentration and inversely proportional to its temperature. The regenerator, on the other hand, undergoes the inverse process. The hot and diluted desiccant solution (characterised by a high equilibrium vapour pressure) desorbs moisture to the air (which becomes hot and humid and is usually scavenged) and becomes concentrated. Endothermic regeneration can be powered by low-grade heat sources, such as waste heat, solar energy, etc.

Empirical correlations of two parameters, moisture effectiveness and enthalpy effectiveness, based on experimental results and theoretical analysis, have previously been proposed to carry out a quick performance prediction and preliminary design of the dehumidifier and regenerator. These parameters are simple to incorporate into energy and mass balance equations for predicting the performance of liquid desiccant technology. The moisture effectiveness, ϵ_{ω} , is defined as a dimensionless ratio of the actual moisture content reduction/increase of the air to the maximum potential reduction/increase when the air and the inlet liquid desiccant solution reach an equilibrium state. The moisture effectiveness of the dehumidification and regeneration process is expressed in Eqs. (1) and (2), respectively:

$$\epsilon_{\omega,deh} = \frac{\omega_{a,in} - \omega_{a,out}}{\omega_{a,in} - \omega_{eq,sol}} \quad (1)$$

$$\epsilon_{\omega,reg} = \frac{\omega_{a,out} - \omega_{a,in}}{\omega_{eq,sol} - \omega_{a,in}} \quad (2)$$

where $\omega_{a,in}$ and $\omega_{a,out}$ represent moisture content in the air at the inlet and outlet of the dehumidifier/regenerator, respectively, while $\omega_{eq,sol}$ is the equilibrium moisture content of the inlet solution, defined as the moisture content of the air in equilibrium with the solution.

Similarly, the enthalpy effectiveness, ϵ_h , of the dehumidification and regeneration process is expressed in Eqs. (3) and (4), respectively:

$$\epsilon_{h,deh} = \frac{h_{a,in} - h_{a,out}}{h_{a,in} - h_{eq,sol}} \quad (3)$$

$$\epsilon_{h,reg} = \frac{h_{a,out} - h_{a,in}}{h_{eq,sol} - h_{a,in}} \quad (4)$$

where $h_{a,in}$ and $h_{a,out}$ represent the enthalpy of the air at the inlet and outlet of the dehumidifier/regenerator, respectively, while $h_{eq,sol}$ is the enthalpy of the air in equilibrium with the solution.

3. Scope and methodology

The scope of the research, as shown in Fig. 3, was to develop new correlations for the moisture and enthalpy effectiveness of the dehumidification and regeneration process that could be used to evaluate the performance of the liquid desiccant technology under various operating, outdoor air, desiccant solution and air-solution contact conditions (different packing materials and volumes and flow configurations). The developed correlations not only predict the temperature and humidity control characteristics of the liquid desiccant technology but also aid in estimating its economic performance by associating capital (CAPEX) and

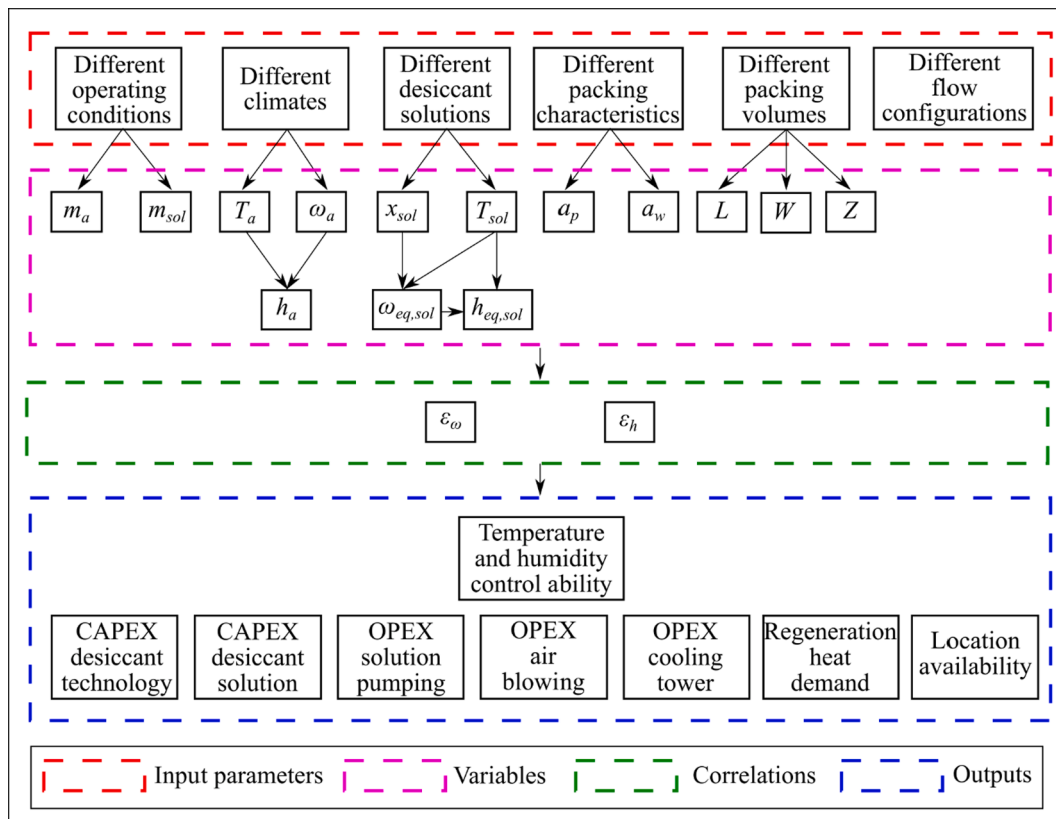


Fig. 3. Scope of the research.

operating (OPEX) expenses of the liquid desiccant process, such as the CAPEX of the liquid desiccant system (which is primarily dependent on the air volume flow rate, V_a [40]), the CAPEX of the desiccant solution (once known m_{sol} , x_{sol} and the desiccant salt cost [39]), the OPEX for solution pumping and air blowing (dependent on m_{sol} and m_a), the OPEX of the cooling tower (based on the heat rejection required by the liquid desiccant solution), heat demand for regeneration and location availability. Fig. 3 depicts the relationships between these variables, parameters, correlations and outputs.

Fig. 4 illustrates the framework that was designed and used to develop the best statistically performing correlations for the dehumidification and regeneration processes, which is based on 12 main steps:

- The main correlations found in the literature were reviewed to identify research questions, aims and objectives, as well as to demonstrate the motivation for the research (Steps 1 and 2).
- After describing the liquid desiccant technology and defining the parameters for evaluating effectiveness (Step 3), the research methodology was designed and planned to address the research questions, aims and objectives (Step 4).
- The first step in developing the correlations was to analyse the characteristics, ranges and trends of previously developed correlations (Step 5) to highlight the most important factors in terms of heat and mass transfer, packing material (material, geometry and

wetting) and flow configuration (Step 6) and determine which parameters to include in the newly developed correlations.

- After determining the main parameters influencing the moisture and enthalpy effectiveness, experimental data were collected and screened. The data were primarily gathered from 176 sets of dehumidification experimental data and 92 sets of regeneration experimental data from 9 and 6 published papers, respectively, that used different liquid desiccants, such as LiCl and LiBr, in cellulose structured packed bed with cross-flow or counter-flow flow patterns (Step 7).
- Using the collected experimental data, different multiple regression models (linear and nonlinear) were tested and their predictive ability was compared (Step 8). As reported by Wen and Lu [24] for the study of liquid desiccant processes, the accuracy of the effectiveness correlations can be evaluated by calculating their mean absolute relative deviation, MARD, as defined in Eq. (5):

$$MARD = \frac{1}{N} \sum_{i=1}^N \left| \frac{\epsilon_{calc} - \epsilon_{exp}}{\epsilon_{exp}} \right| * 100\% \quad (5)$$

where ϵ_{calc} and ϵ_{exp} are the calculated and experimental moisture or enthalpy effectiveness of the dehumidification or regeneration process evaluated for N experimental points, respectively. In addition, the residuals, r , of regression models were analysed to assess the difference between measured and calculated values [41]. The residual standard

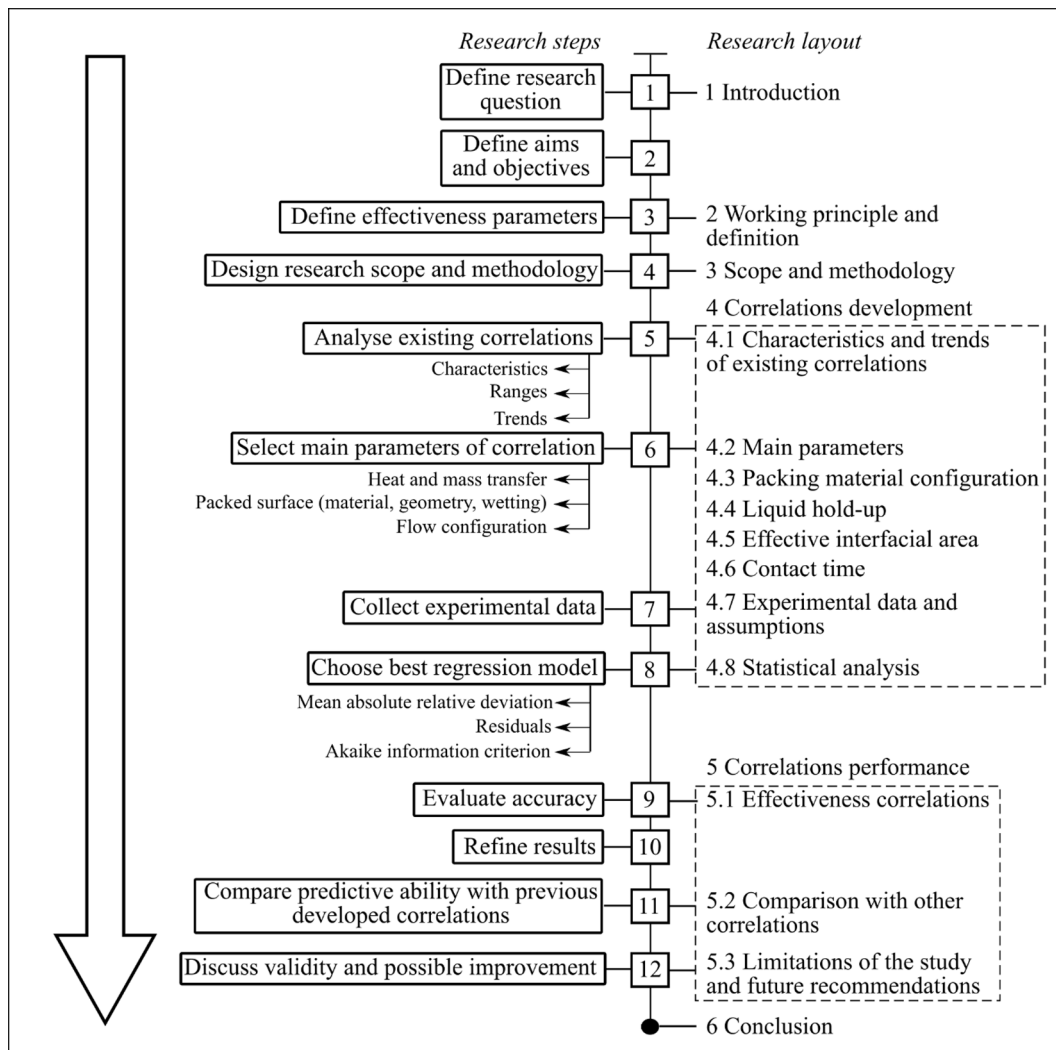


Fig. 4. Framework of research steps and corresponding research layout.

deviation, S_{res} , was calculated to compare the residuals of different models, as shown in Eq. (6):

$$S_{res} = \sqrt{\frac{\sum_{i=1}^N r_i^2}{N-p}} \quad (6)$$

where p is the number of the parameters used in the regression model development. To evaluate the out-of-sample prediction ability and potential overfitting of the regression models and select the model estimated to be the best, the Akaike information criterion, AIC , was also used [42]. For a sample with a reduced size characterised by a ratio between N and p lower than 40 (as in this study), a corrected value of AIC , AIC_C , is used, as shown in Eq. (7) [43]:

$$AIC_C = -2\log(l) + 2p + \frac{2p(p+1)}{(N-p-1)} \quad (7)$$

where l is the maximum likelihood of the regression model. For independent and identically distributed normal errors, $-2 \cdot \log(l)$ equals to $N \cdot \log(SSE/N)$, where SSE is the error sum of squares, calculated as the sum of the squared residuals. Based on information theory, the AIC_C is used to compare non-nested, linear and nonlinear regression models with a different number of parameters by identifying the model that can achieve the best compromise between the best fit and the complexity of the model [42]. The variation in AIC_C between different models, $\Delta AIC_{C,i}$,

was used to estimate the likelihood that a model is correct and quantify this likelihood with a numerical value, being models estimated to be the best characterised by lower values of AIC_C . The parameter can be calculated using Eq. (8):

$$\Delta AIC_{C,i} = AIC_{C,i} - AIC_{C,min} \quad (8)$$

where $AIC_{C,min}$ is the regression model with the lowest value of AIC_C and, as such, estimated to be the best among the regression models for the given data set. Although the calculation of $\Delta AIC_{C,i}$ can be useful for comparing and ranking different regression models, an additional parameter, defined as the Akaike weight, w_i , can be further calculated to quantify the plausibility of the various regression models as a percentage, as shown in Eq. (9) [42]:

$$w_i = \frac{\exp\left(-\frac{1}{2}\Delta AIC_{C,i}\right)}{\sum_{m=1}^M \exp\left(-\frac{1}{2}\Delta AIC_{C,i,m}\right)} \quad (9)$$

where M is the number of regression models that have been compared (7 in this study).

- After determining the best performing regression models and estimating their predictive ability (Step 9), the main factors limiting the

Table 2

Trends and range of correlations for moisture and enthalpy effectiveness of the dehumidification and regeneration process.

	Ref.	$m_{a,in}$ (kg/s)	$m_{sol,in}$ (kg/s)	$T_{a,in}$ (°C)	$T_{sol,in}$ (°C)	$\omega_{a,in}$ (kg/kg)	$x_{sol,in}$ (-)	a_p (m ² /m ³)
Dehumidification	ϵ_ω	[25] ↓	↑	↓	↑	n/a	↑	↑
		$S_a = 0.1-1.2$	$S_{sol} = 6-11$	n/s	n/s	n/s	0.9-0.95	341,465
		[26] ↓	↑	↓	↑	n/a	↑	↓
		$S_a = 0.89$	$S_{sol} = 2.47-3.51$	34-38	33	0.0295	0.375-0.425	465
		[27] ↑	↓	↑	↓	↑	↑	↑
		$S_a = 0.5-1.5$	$S_{sol} = 4.5-6.5$	24-36	24-36	0.011-0.023	0.93-0.96	$a_p Z = 84-262$
		[28] n/a	↑	↓	n/a	n/a	n/a	↓
		$S_a = 1.5-2.613$	$S_{sol} = 0.13-1$	25-45	28-45	n/s	0.93-0.98	77-200
		[20] ↓	↑	n/a	n/a	n/a	n/a	n/a
	$0.41-0.45$	$S_{sol} = 0.34-0.52$	28.2-32.7	21.3-27.8	0.012-0.0161	0.428-0.48	n/s	
	[29] ↑	↓	↑	↓	n/a	↑	n/a	
	$0.31-0.47$	$0.3-0.64$	24.7-33.9	21.1-27.8	0.012-0.016	0.426-0.483	396	
	[30] ↓	↑	↓	↑	n/a	↑↓	n/a	
	$S_a = 0.4-2.04$	$S_{sol} = 0.5-3.25$	26.8-39.2	26.2-38.2	0.0164-0.0245	0.327-0.43	608	
	[31] ↓	↑	n/a	↓	↓	↑	n/a	
	$0.33-0.48$	$0.21-0.56$	25.4-35.4	19.7-27.2	0.0095-0.0182	0.422-0.541	396	
	[31] ↓	↑	n/a	↓	↓	↑	n/a	
	$0.29-0.5$	$0.23-0.42$	25.4-35.4	21.8-29	0.0098-0.0204	0.278-0.367	396	
[32] ↓	↑	n/a	n/a	n/a	n/a	n/a		
$0.08-0.14$	$0.1-0.26$	27-38	22-50	0.0093-0.0213	0.32-0.4	396		
[33] ↓	↑	↓	↓	↑	n/a	n/a		
$0.034-0.082$	$0.023-0.12$	25-40.5	16.4-35.3	0.0106-0.0251	0.317-0.401	650		
ϵ_h	[27] ↑	↓	↑	↓	↑	↑	↑	
	$S_a = 0.5-1.5$	$S_{sol} = 4.5-6.5$	24-36	24-36	0.011-0.023	0.93-0.96	$a_p Z = 84-262$	
	[20] ↓	↑	n/a	n/a	n/a	n/a	n/a	
	$0.41-0.45$	$0.34-0.52$	29.3-29.8	21.2-27.8	0.012-0.0161	0.428-0.48	n/s	
	[32] ↓	↑	↓	↓	↑	=	n/a	
	$0.08-0.14$	$0.1-0.26$	27-38	22-50	0.0093-0.0213	0.32-0.4	396	
[33] ↓	↑	↑	↓	n/a	↓	n/a		
$0.034-0.082$	$0.023-0.12$	25-40.5	16.4-35.3	0.0106-0.0251	0.317-0.401	650		
Regeneration	ϵ_ω	[27] ↑	↓	↑	↓	↑	↑	↑
		$S_a = 0.5-1.5$	$S_{sol} = 4.5-6.5$	30-50	59-71	0.011-0.023	0.93-0.96	$a_p Z = 84-262$
		[35] ↓	↑	↓	↓	↓	↑	n/a
		$0.0052-0.0232$	$0.0016-0.0077$	62.8-112.6	28.2-39.9	0.0116-0.0172	0.393-0.472	n/s
		[36] ↓	↑	n/a	↓	n/a	↑	n/a
	$0.26-0.42$	$0.35-0.63$	28.6-36.4	48.6-62.7	0.012-0.022	0.38-0.54	396	
	[31] ↓	↑	n/a	↓	↑↓	↑	n/a	
	$0.24-0.4$	$0.26-0.48$	30.3-36.6	48.5-59.4	0.0105-0.022	0.422-0.541	396	
	[31] ↓	↑	n/a	↓	↑↓	↑	n/a	
	$0.24-0.4$	$0.26-0.48$	30.3-36.6	48.5-59.4	0.0105-0.022	0.237-0.407	396	
ϵ_h	[27] ↑	↓	↑	↓	↑	↑	↑	
	$S_a = 0.5-1.5$	$S_{sol} = 4.5-6.5$	30-50	59-71	0.011-0.023	0.93-0.96	$a_p Z = 84-262$	

↑ Parameter increases with the variable; ↓ Parameter decreases with the variable; = Marginal or no change at all; ↑↓ Parameter changes irregularly with variable; n/a Parameter was not available in the correlation; n/s Range of parameter was not specified.

predictive ability were identified and a refined result for a narrower range of flow rates was obtained (Step 10).

- A comparison of the accuracy of the newly developed correlations with those available in the literature complemented the research (Step 11), which is concluded with a discussion of the accuracy and validity of the obtained results for future research (Step 12).

4. Correlations development

4.1. Characteristics and trends of existing correlations

Table 2 presents the predicting abilities of the correlations listed in Table 1 for the dehumidification and regeneration process. Table 2 was created by calculating these correlations in MATLAB and evaluating their performance with the variation of the main parameters of the liquid desiccant process, considering LiCl as the desiccant solution [44].

Key points drawn from Table 2 are as follow:

- (1) The flow rate, m_{sol} and m_a , and the temperature, T_{sol} and T_a , of the solution and the air are used in the majority of the correlations.
- (2) Moisture absorption/desorption performance is expressed by the mass fraction of desiccant salt in the solution, x_{sol} , in some correlations, such as those proposed by Liu *et al.* [29,31,36]. However, the ability of a desiccant solution to absorb/desorb moisture is determined by its equilibrium moisture content, $\omega_{eq,sol}$, rather than its mass fraction. Different desiccant solutions with the same mass fraction have, in general, different moisture absorption/desorption characteristics. As such, more universal parameters for the performance of the moisture absorption/desorption process should be used in the correlations.
- (3) The effect of the packing surface contact, a_p , is not considered in most of the correlations. When included, the effect is unclear:
 - the correlation proposed by Abdul-Wahab *et al.* [28] identified an inverse proportionality between a_p and ε_{ω} . However, a higher specific surface area would be helpful to improve the effectiveness of the process.
 - for the correlations proposed by Chung [25] and Chung *et al.* [26], the packing does not significantly affect the performance of the dehumidification process.
 - the correlation proposed by Martin and Goswami [27] is the one that better describes the increase in performance due to the effect of the packing, including the parameters a_p and Z , and is the only one that considers the effect of wetting on the performance, represented by the ratio σ_{sol}/σ_c between the surface tension of the desiccant solution and the critical surface tension of the packing material.
- (4) The only correlations including the packing geometry dimensions are those proposed by Chung [25], Chung *et al.* [26] and Martin and Goswami [27]. These correlations were developed for counter-flow systems and include the height of the packing, Z , as the geometry parameter. In cross-flow dehumidifiers, this strategy would fail to account for the effective geometry of contact. As a result, more universal geometric packing parameters should be used in the correlations.

The learning and analysis of these correlations will be used in the next section for the selection of effective parameters for the development of new correlations.

4.2. Main factors

The performance of the dehumidification and regeneration can be expressed as a function where the main factors affecting the process are indicated, as shown in Table 3:

As discussed in Sections 1 and 4.1, the effect of the packing wetting and size were not included in most of the previously developed

Table 3
Main parameters selection and characteristics.

Main factor	Parameter	Key points
Flow rates	m_a, m_{sol}	<ul style="list-style-type: none"> • Ratio m_{sol}/m_a is a primary factor for the performance of the system. • Secondary effect on pressure drop, wetting of the packing material, electricity consumption of the pumping system, thermo-chemical energy storage ability and air-solution contact time. • Depending on the ventilation or heat load (dependent on m_a), m_{sol} is changed according to the process demand. Optimal m_{sol}/m_a ratios range between 2 and 2.3 [45].
Heat transfer	T_a, T_{sol}	<ul style="list-style-type: none"> • Sensible heat transfer happens due to the difference in temperature between the air and the solution.
Mass transfer	$\omega_a, \omega_{eq,sol}$	<ul style="list-style-type: none"> • The moisture absorption/desorption process is driven by the difference between the vapour pressure of the air (dependent on temperature and moisture content at ambient pressure) and the equilibrium vapour pressure of the desiccant solution, which in turn depends on the temperature and concentration of the solution, which define the equilibrium moisture content of the solution.
Coupled heat and mass transfer	$h_a, h_{eq,sol}$	<ul style="list-style-type: none"> • The absorption/desorption process involves sensible and latent (heat release/intake due to water vaporisation) heat transfer. This coupled effect of the heat and mass transfer process is expressed by the difference between the enthalpy of the moist air and the enthalpy of the air in equilibrium with the solution.
Effect of the packing (geometry, material and configuration)	L, W, H a_p, a_w	<ul style="list-style-type: none"> • An efficient contact between air and the desiccant solution is required to ensure the effectiveness of the heat and mass transfer process in the desiccant system. • Material, geometry and arrangement of the packing play a primary role in the moisture absorption/desorption process. • Hydrodynamics concepts (e.g. hydraulic capacity of the packing determining the diameter of the column) affect the performance of the packing.

correlations. The new correlations developed in this study included a factor to consider them. Additional description of the effect of packing and its wetting on the dehumidification/regeneration process, as well as how to account for it in the correlations is described in the next section.

4.3. Packing material configuration

Five main types of air-desiccant solution contact are found in the literature: packed bed (random or structured), spray type, wetted wall column and membrane-based [46]. Because of its higher performance and lower pressure drop, structured packing has become the most popular choice for desiccant systems, and it is being considered in the correlation development. While structured packing made of ceramic, metal and aluminium have been proved to be less efficient due to their limited wetness [33], cellulose fibre paper has been shown to significantly improve desiccant system performance. Potnis and Lenz [47] demonstrated the adsorbent properties of cellulose as well as its high wettability. Previously employed as pads in direct evaporative coolers [48], CELdek® packing is the most common commercialised cellulose

corrugated sheet structured packing [33].

The sheets of structured packing are typically rotated alternately of 90° to ease the distribution of liquid and improve the contact with the air [49]. The placement of the corrugated elements with different orientations of corrugation creates triangular flow channels between the sheets through which air and solutions flow. Fig. 5 shows an example of corrugated structured packing and the geometry of the flow channel.

The corrugation angle, θ , represents the orientation of the packing corrugation. Characteristic values of θ are 45° or 60° [51]. The inclination of θ influences the performance of the packing and is usually changed according to the application of the packing material. The main geometrical parameters of the packing are the void fraction, e , the specific surface area, a_p , and the equivalent diameter of the packing, d_{eq} [52]. The specific surface area represents the ratio between the area of the packing and the bulk volume of the packing material. Analogously, the void fraction of the packing is the ratio between the volume of the free space of the packing material and the bulk volume of the packing material. For d_{eq} , two definitions are found in the literature [52]. By considering the packing as a system of connected flow cross-sections with different dimensions, d_{eq} equals the average hydraulic diameter of the packing channels. In this study, d_{eq} was calculated as Eq. (10) [52]:

$$d_{eq} = \frac{4e}{a_p} \quad (10)$$

For the simplified geometry of the flow channel shown in Fig. 5, d_{eq} is estimated as the hydraulic diameter of the packing channels, which can also be calculated using the corrugation height, y , the corrugation side length, s , and the corrugation base width, b , of the packing with the corrugation sides covered by a film of liquid, δ [51].

4.4. Liquid hold-up

In the literature, there are several models for studying the influence of structured packing columns, including pressure drop [53,54] and mass transfer estimation [49]. All these models involve the use of a hydrodynamic parameter, the liquid hold-up, H_{liq} , since the surface area available for heat and mass transfer in the system is directly related to the liquid holdup, and particularly to the operating holdup [55]. As a result, estimating the liquid hold-up is critical for assessing the moisture absorption/desorption performance of the structured packing tower. Rocha's assumption, which is valid for corrugated sheet structured

packing [55], was used in the development of the correlations. In his study, Rocha assumed that the flow cross-sections of the packing are a series of inclined wetted wall columns. The geometry of these channels is determined by the corrugation angle and the packing size [56]. In these channels, the desiccant solution and the air are split up and the desiccant solution flows over the packing surface as a film [55].

The total liquid hold-up, H_{liq} , represents the volume of the liquid present in the whole volume of the packing material (m^3/m^3). This parameter is influenced by the thermodynamic properties of the fluid, as well as the geometry and composition of the packing material [56]. The total holdup is the sum of its static and dynamic components. The static hold-up, H_{sb} , represents the liquid that remains in the packing surface due to capillary forces when the flow of liquid to the packing material is stopped. While its calculation adds complexity to the hydrodynamic study of the packing, the static holdup is usually negligible in comparison to the total holdup [55] and as such it will not be considered further in this study. The operating hold-up, H_{op} , represents the liquid that drains from the packing when the supply of liquid is interrupted. For a packed column in operation, this value is directly proportional to the flow of liquid through the packing [57]. For the structured packing, H_{op} can be calculated using Eq. (11) [58]:

$$H_{op} = C a_p^{0.83} q_{sol}^B \left(\frac{\mu_{sol}}{\mu_w} \right)^{0.25} \quad (11)$$

where C and B are two constants equal to 0.000051 and 0.6 for cellulose packing, respectively, a_p is specific area per unit volume of the packing (m^2/m^3), q_{sol} is volumetric flux of desiccant solution ($m^3/(m^2 \cdot h)$), μ_{sol} is dynamic viscosity of desiccant solution ($mPa \cdot s$), μ_w is dynamic viscosity of water at $20^\circ C$ ($mPa \cdot s$).

Suess and Spiegel proposed Eq. (11) for H_{op} in the region below the loading point [59]. The loading point for packed columns is the operating condition where the air velocity is high enough to start restricting liquid flow [60]. For a constant flow rate of desiccant solution, the pressure drop increases proportionally to the air velocity. When the loading point is reached, the liquid desiccant fills the voids in the packing (significantly increasing the pressure drop and reducing the heat and mass transfer capacity) until the flooding point is reached, at which the air velocity is high enough to carry away all of the solution from the packing tower [61]. Below the loading point, H_{op} is mostly dependent on the solution flow rate and remains relatively constant as U_a varies. When the air velocity exceeds the loading point, there is a significant increase in pressure drop and, as a result, electricity

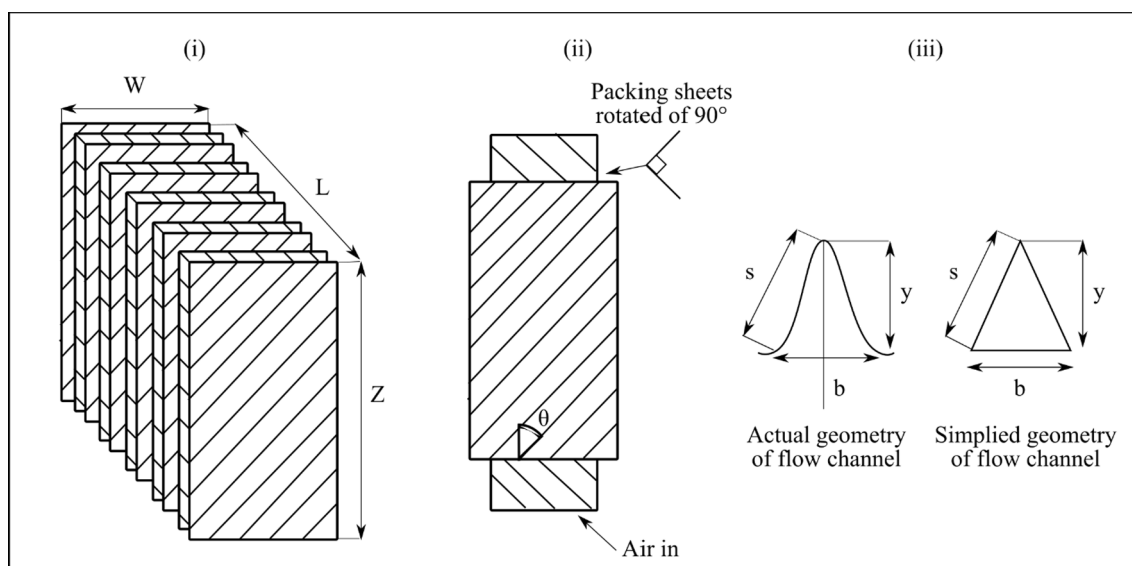


Fig. 5. Schematic diagram of (i) structured packing, (ii) corrugation angle of sheets and (iii) geometry of flow channel, adapted from [50].

consumption. As a result, it should be strictly avoided in desiccant systems. The recommended air velocity is 80–90% of the loading point [61]. In this condition, the operating hold-up is a parameter that can be used to evaluate the heat and mass transfer in the packing material and it was used for the development of the correlations. It is important to note that the coefficient of the Suess-Spiegel model must be determined for various types of packing using the traditional volumetric method, which involves conducting an experiment with a calibrated tank to collect the drain that falls out of the packing when the liquid supply is interrupted [16,58]. In their paper, Suess and Spiegel evaluated these coefficients for metal sheet structured packing [59]. In recent years, Kabeel *et al.* estimated the operating hold-up using the Suess-Spiegel model for CELdek® packing 7090 [58], while Wang *et al.* for CELdek® 5090 [16]. These two types of cellulose packing material were considered in the development of the correlations in this study.

4.5. Effective interfacial area

After calculating the liquid holdup, the effective interfacial area of the structured packing [56] can be determined, which is another important factor in determining how well the packing material wets and performs in terms of coupled heat and mass transfer. There are several definitions of effective interfacial area in the literature [62]. For packed bed liquid desiccant dehumidifiers and regenerators, the effective interfacial area is defined as the contact surface between air and desiccant solution that is actually wetted and actively participates in heat and mass transfer [58,63], which is primarily dependent on the packing characteristics (material and geometry), the thermodynamics of the desiccant solution (density, viscosity and surface tension) and the operating condition of the system [4].

In the literature, various correlations for estimating the effective interfacial area of random [8,64] and structured packing [65,66] have been proposed. Brunazzi *et al.* [67] developed a correlation for the ratio between effective interfacial area and surface-to-volume ratio. Based on a wetted wall column model similar to Rocha's, the model assumes a flow of liquid solution down an inclined tube of the structured packing as a laminar falling film with thickness δ [62,68]. In this study, the interfacial area between the desiccant solution and the air is assumed to be equal to the effective surface area [62]. Because of this assumption, the liquid holdup can be used to estimate the effective (wetted) area of the cellulose structured packing, a_e , as shown in Eq. (12) [67]:

$$\frac{a_e}{a_p} = \left(\frac{d_{eq}}{4}\right) \left(\frac{H_{op}}{e}\right)^{1.5} \left(\frac{\rho_{sol} e g \sin^2 \theta}{3\mu_{sol} U_{sol}}\right)^{0.5} \quad (12)$$

where θ is the corrugation angle, H_{op} is the operating holdup (m^3/m^3) and U_{sol} is the velocity of the desiccant solution. Eq. (12) will be used to account for the effect of packing wetting on performance in the newly derived correlations.

4.6. Contact time

In addition to the wetting characteristics of the packing material, the dimensions of the packing have a significant influence on the heat and mass transfer process. According to Dong *et al.* [69], the contact time between air and desiccant solution, which is related to the dimensions of the packing, has a major impact on the performance of the system. For various desiccant system flow patterns, this parameter, which is affected by packing size and air velocity, can be defined as follows:

$$t = \frac{j}{U_a} \quad (13)$$

where t is air-desiccant contact time (s), j is the crossing length of air which is equal to Z (m) and L (m) for counter- and cross-flow configurations, respectively, and U_a is air flow velocity (m/s). By including the contact time in the correlations, an equation can be found that predicts

the performance of both counter- and cross-flow patterns.

4.7. Experimental data and assumptions

For the regression of the correlations, experimental data of the dehumidification (176 points) and regeneration (92 points) process were collected and analysed from 9 and 6 papers, respectively, as summarised in Table 4. A complete list of the experimental data used in the analysis can be found in Appendix B.

The liquid holdup of the packing material is estimated using hydrodynamic parameters, such as a_p , ε , θ , *etc.* When these values are not available, d_{eq} is computed based on the height, length and side of the packing equivalent geometry, as shown in Fig. 5, and then used to calculate the other parameters. When these factors are not available, they were derived from similar cases in the literature. Table 5 shows the values used in the development of the correlations for the hydrodynamic parameters of the packing [70,71].

The following assumptions were taken into account when developing the correlations:

- The liquid desiccant system worked in preloading conditions (U_a is lower than the loading point).
- The equation for the wetting of the packing was applied to corrugated sheet cellulose.
- Thermodynamic functions of moist air were modelled based on Ref. [77].
- Thermodynamic functions of desiccant solutions were modelled based on Refs. [44,78].

4.8. Statistical analysis

The inlet predictors shown in Eq. (14) were chosen for the regression analysis in accordance with the research scope and analysis of the main factors involved in the process, as described in Sections 4.1–4.6.

$$\begin{cases} X_1 = \frac{m_{sol}}{m_a} \\ X_2 = \frac{T_{sol,K}}{T_{a,K}} \\ X_3 = \frac{h_{eq,sol}}{h_a} \\ X_4 = \frac{\omega_{eq,sol}}{\omega_a} \\ X_5 = t \\ X_6 = \frac{a_e}{a_p} \end{cases} \quad (14)$$

To evaluate and select the better performing correlations, various linear and nonlinear regression models were tested for regression using the gathered experimental data, as shown in Table 6.

5. Correlations performance

5.1. Effectiveness correlations

Based on the analysis of $MARD$, S_{Res} and AIC_C , the better performing correlations for the moisture and enthalpy effectiveness of the dehumidification and regeneration process in the application range illustrated in Table 4 were identified, as summarised in Table 7, where $Rel10$ and $Rel20$ represent the percentage of data points falling within the $\pm 10\%$ and $\pm 20\%$ difference between measured and estimated effectiveness, respectively. Appendix C contains the complete equations for the developed correlations as well as a complete analysis of their predictive ability.

In regard to the dehumidification process, all the experimental data collected for moisture and enthalpy effectiveness were used to fit the

Table 4
Ranges of the full set of experimental data used for the correlation development.

Parameter	Dehumidification		Regeneration	
	ϵ_w	ϵ_h	ϵ_w	ϵ_h
Data points	176	135	92	92
Paper number	9	8	6	6
m_{sol}/m_a (-)	0.096–14.14	0.096–14.14	0.125–5.43	0.125–5.43
T_a (°C)*	21.7–39	21.7–39	4.42–46.72	4.42–46.72
T_{sol} (°C)*	9.5–32.17	9.5–32.17	33.5–61	33.5–61
ω_a (kg _{H2O} /kg _{da})	0.0108–0.0318	0.0108–0.0318	0.0023–0.0213	0.0023–0.0213
ω_{sol} (kg _{H2O} /kg _{da})	0.003–0.011	0.003–0.011	0.0097–0.0646	0.0097–0.0646
Z (m)	0.2–2.1	0.2–2.1	0.4–2.1	0.4–2.1
L (m)	0.1–1	0.1–1	0.1–0.4	0.1–0.4
W (m)	0.2–0.75	0.2–0.75	0.2–0.35	0.2–0.35
t (s)	0.15–1.825	0.15–1.3	0.0431–1.486	0.0431–1.486
a_p (m ² /m ³)	396–650	396–650	396–550	396–550
a_e/a_p (-)	0.0866–0.5018	0.0896–0.5018	0.088–0.463	0.088–0.463

* In the correlation development, the temperature was converted from °C to K and applied to the regression model.

Table 5
Geometrical characteristics of structured packing used in correlations development.

Ref.	Chung et al. [9]	Wang et al. [33]	Zhang et al. [50] ^a	Chen et al. [11]	Tang et al. [72]	Liu et al. [31] ^a	Xie et al. [73] ^a	Mohamed et al. [74]	Wang et al. [75] ^b	Varela et al. [76] ^a
L	0.0182/W ^c	0.3	0.25	0.75	0.365	0.3,0.33,0.4	0.16 ^c	0.5,1	0.3	0.1
W	0.0182/L ^c	0.3	0.27	0.75	0.365	0.35	0.16 ^c	0.4	0.3	0.2
Z	0.4	0.3,0.4,0.5	0.5	1.75	0.2,0.3	0.55	2.1	0.4	0.45	0.4
a_p	410	650	550	450	396	396	396	400	410	460
ϵ	0.738	0.9	0.83875	0.9	0.88	0.88	0.88	0.88	0.88	0.851
d_{eq}	0.0072	0.0055	0.0061	0.008	0.009	0.009	0.009	0.088	0.0858	0.0074
θ	45	45	60	60	60	45	45	60	45	45

^a Experimental points for both the dehumidification and the regeneration process; ^b Experimental points only for the regeneration process; ^c Only area was specified.

Table 6
Linear and nonlinear regression models used for correlations development.

	Regression model	Function	Constants required
Linear	Linear	$Y = c_0 + \sum_{i=1}^6 c_i X_i$	7
	Transformed inverse	$1/Y = c_0 + \sum_{i=1}^6 c_i (1/X_i)$	7
	Transformed squared	$\sqrt{Y} = c_0 + \sum_{i=1}^6 c_i \sqrt{X_i}$	7
	Transformed logarithmic	$\log(Y) = c_0 + \sum_{i=1}^6 c_i \log(X_i)$	7
Nonlinear	Power	$Y = c_0 \prod_{i=1}^6 X_i^{c_i}$	7
	Logarithmic	$Y = c_0 + \sum_{i=1}^6 c_i \log(X_i)$	7
	Quadratic	$Y = c_0 + \sum_{i=1}^6 c_i X_i + c_{i+6} X_i^2$	13

Table 7
Best performing regression models for correlations of moisture and enthalpy effectiveness of the dehumidification and regeneration process regressed with the full set of data.

Parameter	Best regression model	MARD (%)	Rel10 (%)	Rel20 (%)	S_{Res}	w_i (%)
$\epsilon_{w,Deh}$	Logarithmic	9.14	68.75	89.77	0.061	66.41
$\epsilon_{h,Deh}$	Transformed inverse	8.47	70.37	90.37	0.056	34.35
$\epsilon_{w,Reg}$	Power	14.54	52.17	78.26	0.08	51.18
$\epsilon_{h,Reg}$	Power	9.2	69.57	83.7	0.059	54.15

correlations. Figs. 6 and 7 show the comparison of measured values with those derived from new correlations for ϵ_w and ϵ_h , respectively. Similarly, all 92 experimental data points gathered in regard to the regeneration process were used to fit the correlations. Figs. 8 and 9 show the comparison between the measured values and those obtained from the new correlations for ϵ_w and ϵ_h , respectively. The data points in the areas

defined by the dashed and dotted lines (referred to as Zone 1 and Zone 2) in Figs. 6–9 have an average error between measured and calculated values of less than or equal to 10% and 20%, respectively.

Regardless of the type of solution or flow pattern, Table 7 reveals that the developed correlations are fairly capable of predicting both moisture and enthalpy effectiveness of the dehumidification process (lower than 10% error). The correlation is less accurate in predicting moisture effectiveness of the regeneration process (the average error is slightly lower than 15%), while the accuracy of the correlation of the enthalpy effectiveness is satisfactory (lower than 10% error).

From the analysis of the differences between the predicted and the calculated effectiveness of the experimental data, it was observed that these were particularly significant at lower effectiveness values, corresponding to systems operating with low m_{sol}/m_a ratios (i.e. low-flow operating zone) and for experiments where the packing material was not specified as cross-corrugated cellulose. Therefore, it is reasonable to narrow down the experimental data to have a better fitting for more practical operational conditions. Compared to the full range of experimental data, better fitting was obtained when only m_{sol}/m_a ratios higher than 0.5 and CELdek® cellulose structured packing were considered, with experimental data reduced to 124 and 52 points for the dehumidification and regeneration process, respectively. The threshold value of 0.5 for m_{sol}/m_a was selected based on previous work done by Factor and Grossman [79], which identified 0.5 as the minimum value of the optimal range of solution-to-air flow ratios. Table 8 shows the characteristics of the reduced experimental points used for the development of the correlations.

The better performing correlations for the reduced set of data are shown in Table 9, while Table 10 shows the regressed coefficients, C_1 – C_7 , for the moisture and enthalpy effectiveness coefficients.

The performance of the newly developed correlations for the dehumidification and the regeneration process in the application range illustrated in Table 8 is increased, as shown in Table 9. For the dehumidification process, both the moisture and enthalpy effectiveness

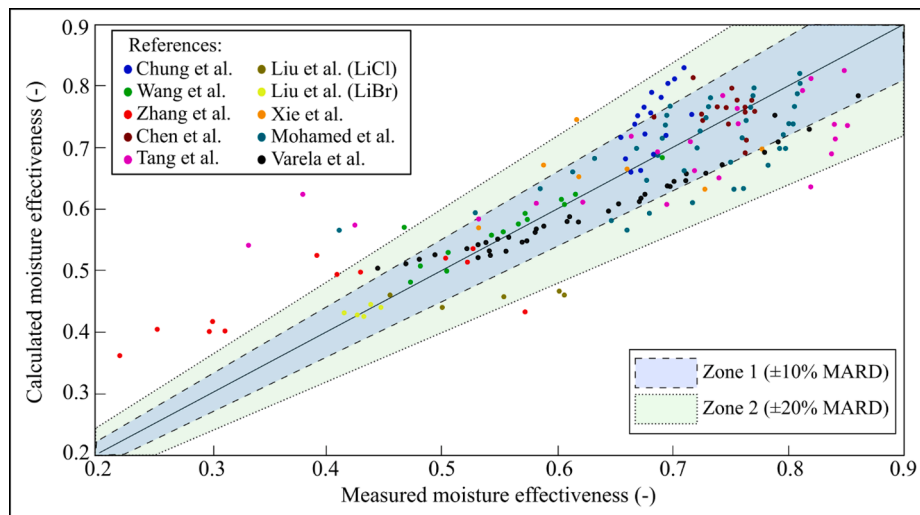


Fig. 6. Comparison of the measured and the estimated moisture effectiveness of the dehumidification process for the whole set of data.

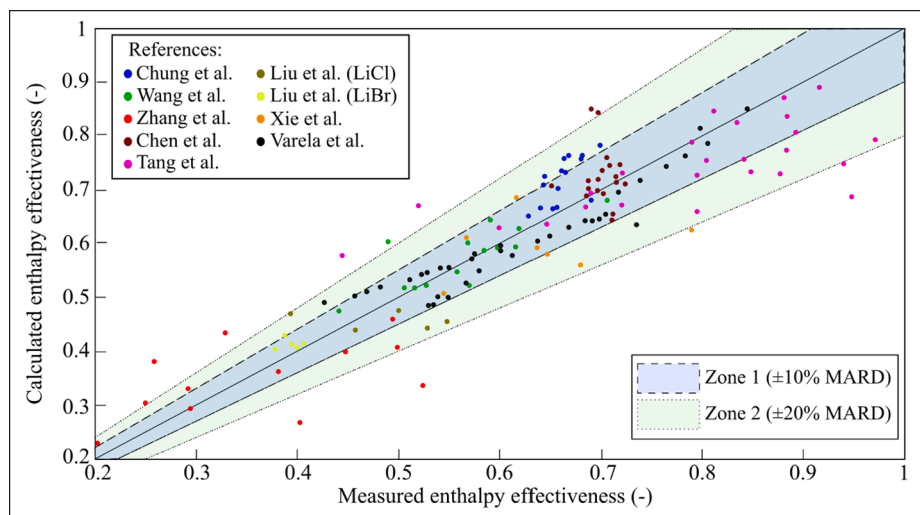


Fig. 7. Comparison of the measured and the estimated enthalpy effectiveness of the dehumidification process for the whole set of data.

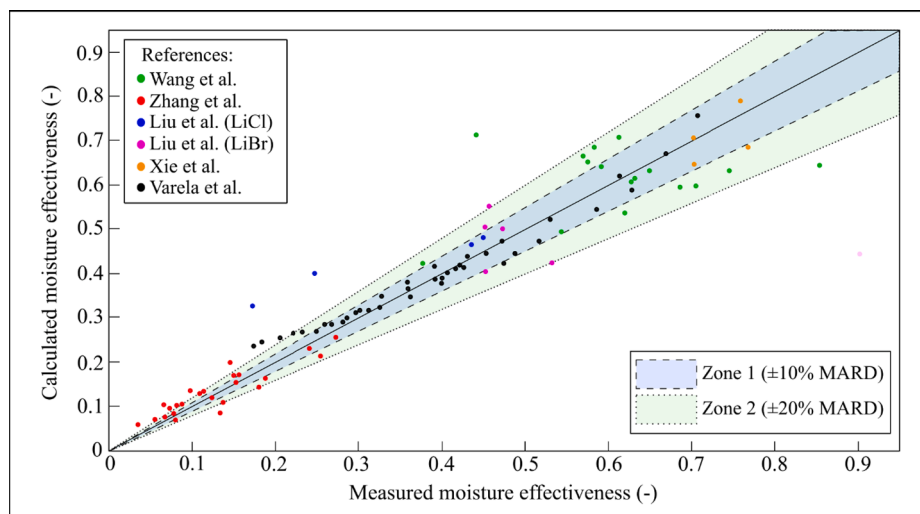


Fig. 8. Comparison of the measured and the estimated moisture effectiveness of the regeneration process for the whole set of data.

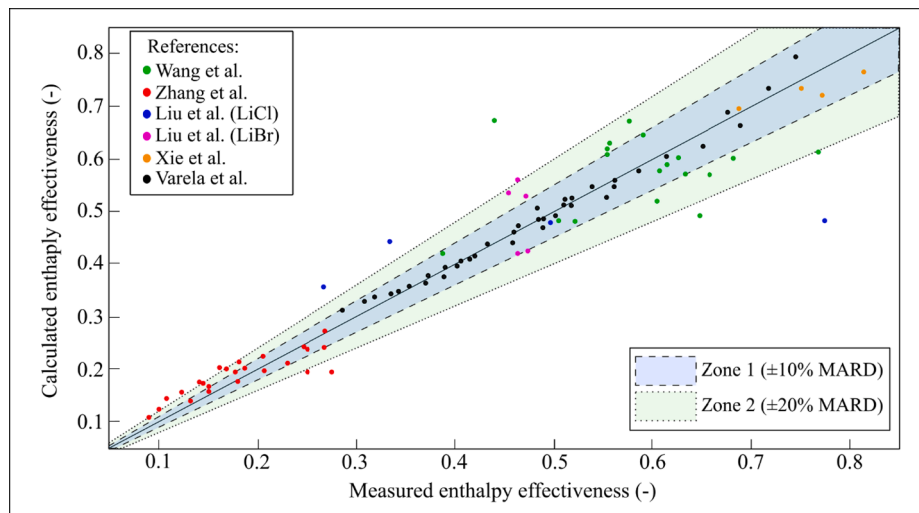


Fig. 9. Comparison of the measured and the estimated enthalpy effectiveness of the regeneration process for the whole set of data.

Table 8

Ranges of the reduced experimental data used for the correlation development.

Parameter	Dehumidification		Regeneration	
	ϵ_w	ϵ_h	ϵ_w	ϵ_h
Data points	124	123	52	52
Paper number	7	7	3	3
m_{sol}/m_a (-)	0.565–14.14	0.565–14.14	0.647–5.43	0.647–5.43
T_a (°C)*	21.7–39	21.7–39	16.9–46.72	16.9–46.72
T_{sol} (°C)*	9.5–32.17	9.5–32.17	33.5–58.5	33.5–58.5
ω_a (kg _{H2O} /kg _{da})	0.0108–0.0318	0.0108–0.0318	0.0107–0.0213	0.0107–0.0213
ω_{sol} (kg _{H2O} /kg _{da})	0.0033–0.011	0.0033–0.011	0.0164–0.0543	0.0164–0.0543
Z (m)	0.2–2.1	0.2–2.1	0.4–2.1	0.4–2.1
L (m)	0.1–0.75	0.1–0.75	0.1–0.4	0.1–0.4
W (m)	0.2–0.75	0.2–0.75	0.2–0.35	0.2–0.35
t (s)	0.15–1.3	0.15–1.3	0.435–1.272	0.435–1.272
a_p (m ² /m ³)	396–650	396–650	396–460	396–460
a_e/a_p (-)	0.145–0.502	0.145–0.502	0.286–0.463	0.286–0.463

* In the correlation development, the temperature was converted from °C to K and applied to the regression model.

Table 9

Best performing regression models for correlations of moisture and enthalpy effectiveness of the dehumidification and regeneration process regressed with the reduced set of data.

Parameter	Best regression model	MARD (%)	Rel10 (%)	Rel20 (%)	S_{Res}	w_i (%)
$\epsilon_{w,Deh}$	Logarithmic	7.2	79.84	94.35	0.064	45.84
$\epsilon_{h,Deh}$	Transformed inverse	6.4	80.49	95.12	0.063	90.14
$\epsilon_{w,Reg}$	Logarithmic	9.18	65.38	90.38	0.074	86.82
$\epsilon_{h,Reg}$	Logarithmic	5.58	86.54	94.23	0.048	79.39

correlations showed an average error lower than 8%, with about 95% of the considered experimental points falling within the 20% range of error. For the regeneration process, the moisture effectiveness showed a higher average error than the dehumidification process (9.18%) with approximately 90% of the considered experimental points falling within

Table 10

Coefficients regressed for the best performing correlation with the reduced set of data.

Parameter	C ₁	C ₂	C ₃	C ₄	C ₅	C ₆	C ₇
$\epsilon_{w,Deh}$	0.751	0.0256	6.4796	-0.9992	0.3703	0.1118	0.1454
$\epsilon_{h,Deh}$	-11.199	0.4352	13.166	-1.0751	0.2998	0.1076	0.0132
$\epsilon_{w,Reg}$	0.9835	0.1477	2.905	-0.835	0.097	0.1383	0.0753
$\epsilon_{h,Reg}$	0.742	0.1637	-0.9174	0.4759	-0.6189	0.0928	-0.0573

the 20% range of error. For the enthalpy effectiveness, the correlation showed high accuracy with an average error of 5.58% and 94.23% of the experimental points falling within the 20% range of error. Figs. 10–13 show the comparison between the measured values and those obtained from the new correlations with the reduced set of data points for ϵ_w and ϵ_h of the dehumidification and regeneration process.

Although the correlations for the moisture and enthalpy effectiveness of the regeneration process showed, in general, a good predictive ability, it is clear from Figs. 12 and 13 that the presence of an outlier, which could be due to a measurement error, has an impact on their predictive ability. Instead of using the least square method, an alternative regression technique, such as robust regression, could be used to reduce the impact of the outlier on the predictive ability of the regression model. Robust regression works by using the iteratively reweighted least squares method and assigning a weight to each data point, making the regression less sensitive to large variations in small parts of the data [80]. Table 11 shows the performance of the correlations regressed for

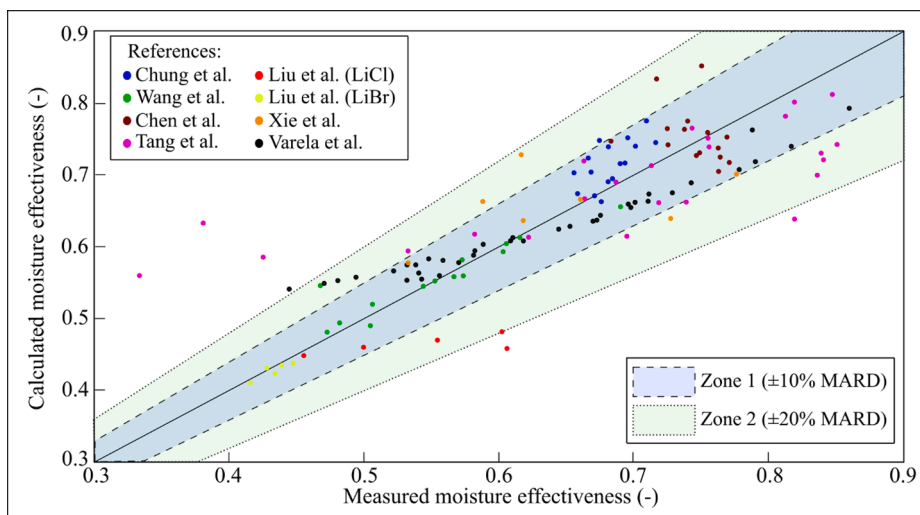


Fig. 10. Comparison of the measured and the estimated moisture effectiveness of the dehumidification process for the reduced set of data.

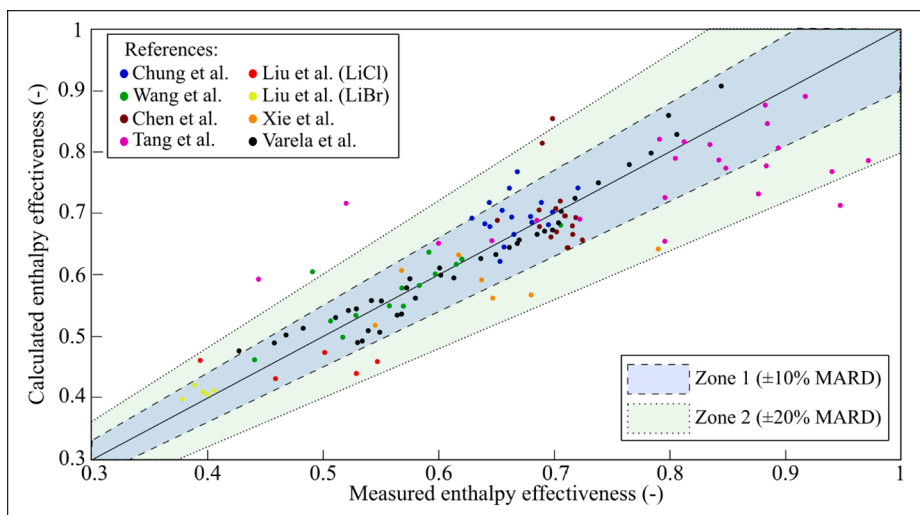


Fig. 11. Comparison of the measured and the estimated enthalpy effectiveness of the dehumidification process for the reduced set of data.

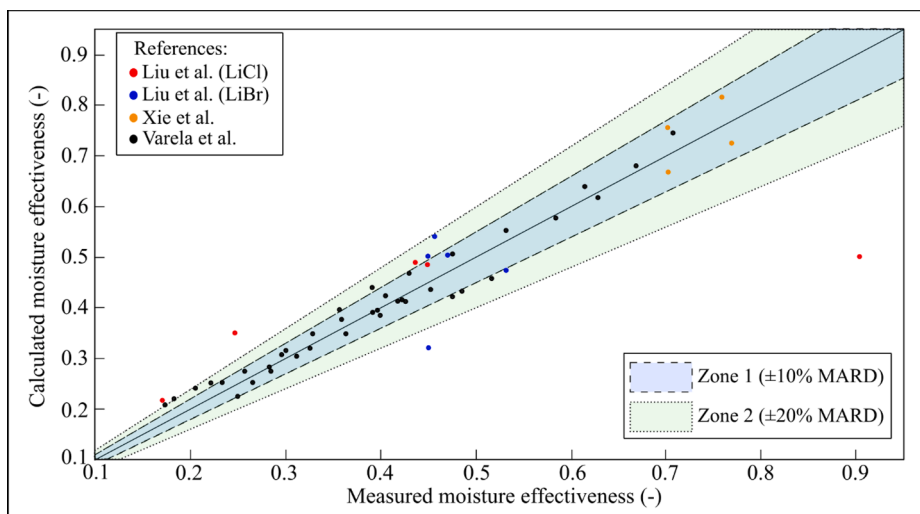


Fig. 12. Comparison of the measured and the estimated moisture effectiveness of the regeneration process for the reduced set of data.

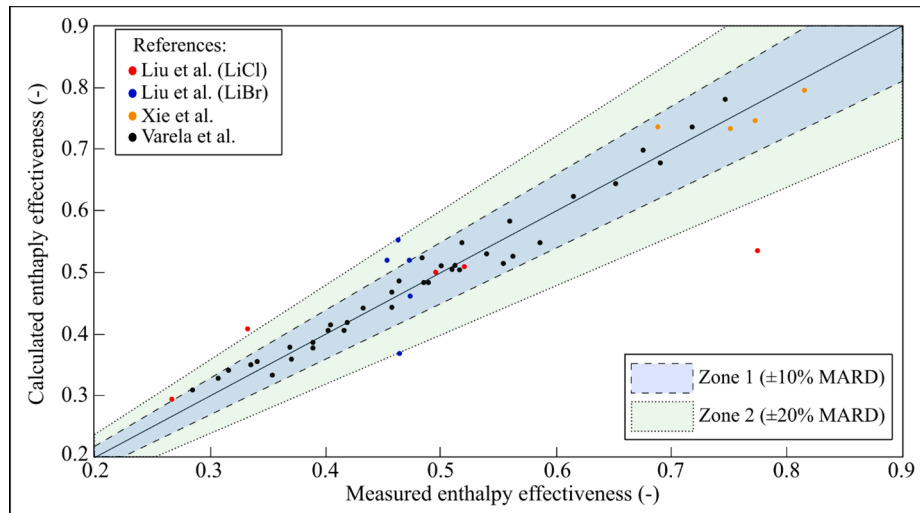


Fig. 13. Comparison of the measured and the estimated enthalpy effectiveness of the regeneration process for the reduced set of data.

Table 11

Best performing regression models for correlations of moisture and enthalpy effectiveness of the regeneration process regressed with robust regression from the reduced set of data.

Parameter	Best regression model	MARD (%)	Rel10 (%)	Rel20 (%)
$\epsilon_{\omega,Reg}$	Logarithmic	6.31	88.46	92.31
$\epsilon_{h,Reg}$	Logarithmic	4.37	92.31	94.23

the regeneration process with a non-linear logarithmic model using robust bi-square regression, while Figs. 14 and 15 show the comparison of the measured and calculated effectiveness of the regeneration process. The full equations of the best performing regressed correlations for the dehumidification and regeneration process are shown in Eq. (15).

$$\begin{cases}
 \epsilon_{\omega,Deh} = 0.751 + 0.026\log\left(\frac{m_{sol}}{m_a}\right) + 6.48\log\left(\frac{T_{sol,K}}{T_{a,K}}\right) - 0.999\log\left(\frac{h_{eq,sol}}{h_a}\right) + 0.37\log\left(\frac{\omega_{eq,sol}}{\omega_a}\right) + 0.112\log(t) + 0.145\log\left(\frac{a_e}{a_p}\right) \\
 1/\epsilon_{h,Deh} = -11.199 + 0.4352\left(\frac{m_a}{m_{sol}}\right) + 13.166\left(\frac{T_{a,K}}{T_{sol,K}}\right) - 1.0751\left(\frac{h_a}{h_{eq,sol}}\right) + 0.2998\left(\frac{\omega_a}{\omega_{eq,sol}}\right) + 0.1076\left(\frac{1}{t}\right) + 0.0132\left(\frac{a_p}{a_e}\right) \\
 \epsilon_{\omega,Reg} = 1.0266 + 0.1645\log\left(\frac{m_{sol}}{m_a}\right) + 0.2034\log\left(\frac{T_{sol,K}}{T_{a,K}}\right) + 0.221\log\left(\frac{h_{eq,sol}}{h_a}\right) - 0.636\log\left(\frac{\omega_{eq,sol}}{\omega_a}\right) + 0.102\log(t) + 0.193\log\left(\frac{a_e}{a_p}\right) \\
 \epsilon_{h,Reg} = 1.1 + 0.155\log\left(\frac{m_{sol}}{m_a}\right) - 5.187\log\left(\frac{T_{sol,K}}{T_{a,K}}\right) + 0.912\log\left(\frac{h_{eq,sol}}{h_a}\right) - 0.9855\log\left(\frac{\omega_{eq,sol}}{\omega_a}\right) + 0.073\log(t) + 0.1375\log\left(\frac{a_e}{a_p}\right)
 \end{cases} \tag{15}$$

5.2. Comparison with other correlations

To further evaluate the predictive ability of the developed correlations, a comparison of the accuracy with those available from the literature was conducted. Table 12 shows the MARD of different correlations for prediction of the moisture effectiveness of the dehumidification process.

Table 12 indicated that some of the correlations were only able to efficiently predict their own experimental data, which was in agreement with [24]. Apart from the newly developed correlation, the correlations of Moon et al. [30] (MARD = 16.98%) and Wang et al. [33]

(MARD = 20.09%) were the ones with higher prediction accuracy. Fig. 16 shows the comparison of the newly developed correlation with those of Moon et al. [30] and Wang et al. [33].

Similarly, Table 13 shows the MARD of different correlations for prediction of the enthalpy effectiveness of the dehumidification process for experimental points obtained for specific desiccant solutions and flow patterns and reported as Refs. in Table 13.

Apart from the newly developed correlation, Wang et al.'s correlation [33] was the one that best predicted the behaviour of the coupled heat and mass transfer in the dehumidifier (MARD = 27.4%). Although being very effective in validating its own experimental data (MARD = 4.11%), the predictive ability of the correlation from Wang et al. [33] dropped for other experimental points. Fig. 17 compares the predictive ability of the newly developed correlation with that of Wang et al. [33], from which it is clear the higher accuracy of the newly developed correlation since Wang et al.'s correlation [33] showed values of enthalpy effectiveness higher than 1 or underestimated.

For the regeneration process, fewer correlations were available for comparison. Table 14 shows the MARD of the various correlations developed for predicting the moisture effectiveness of the regeneration process for experimental points obtained for specific desiccant solutions and flow patterns and reported as Refs. in Table 14.

As shown in Table 14, the previously reported correlations presented unsatisfactory behaviour, with in some cases negative effectiveness. Liu et al.'s correlation [36] is the best performing one with an average error of 38%. Fig. 18 shows the comparison of the predictive ability of the newly developed correlation compared with that of Liu et al. [36], identifying how the latter underestimated the moisture effectiveness of

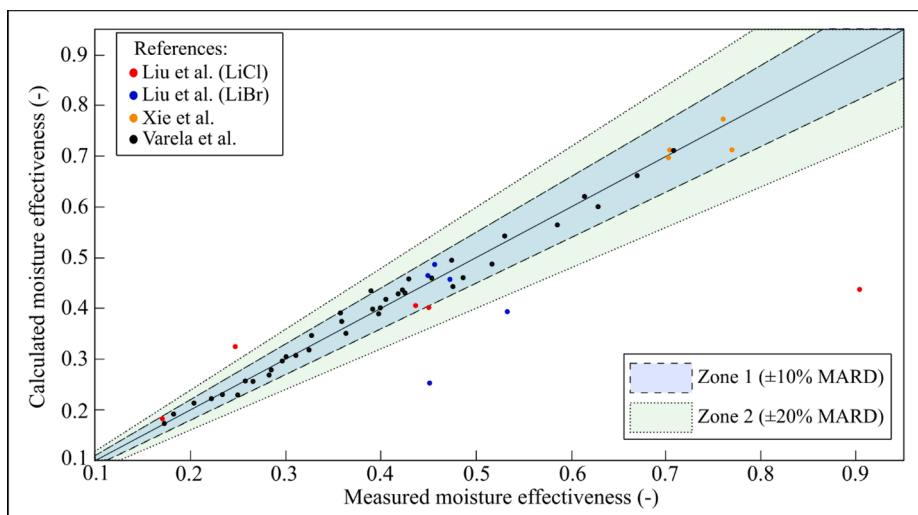


Fig. 14. Comparison of the measured and the estimated moisture effectiveness of the regeneration process regressed with robust technique for the reduced set of data.

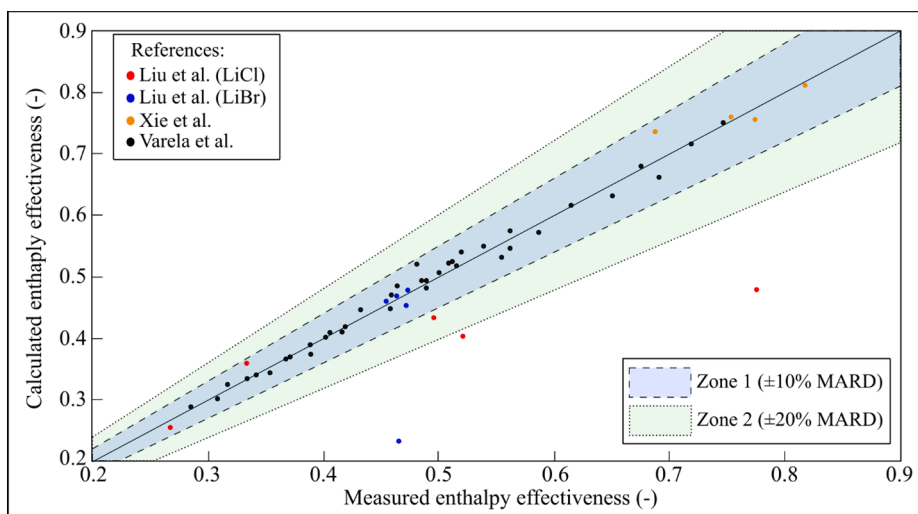


Fig. 15. Comparison of the measured and the estimated enthalpy effectiveness of the regeneration process regressed with robust technique for the reduced set of data.

Table 12

Performance of correlations for moisture effectiveness of the dehumidification process.

Ref.	N*	Liquid desiccant	Flow pattern	MARD (%) of different correlations taken from								
				[25]	[26]	[27]	[28]	[29]	[30]	[32]	[33]	In this study
[9]	16	LiCl	Counter-flow	34.77**	71	66.34	316.5	52.24	11.28	105.4	60.56	5.02
[33]	14	LiCl	Counter-flow	55.12	77.12	26.33	88.79	93.5	11.39	15.68	3.28	2.83
[11]	15	LiCl	Cross-flow	24.16	42.85	4.25	71.2	41.29	18.25	7.71	21.21	5.66
[72]	24	LiCl	Counter-flow	38.83	74.67	142.7	69.64	59.51	21.62	27.18	18.18	13.44
[31]	5	LiCl	Cross-flow	65.64	96.39	14.73	30.37	95.4	12.02	11.14	21.04	13.98
[31]	5	LiBr	Cross-flow	98.49	137.1	24.86	94.16	147.2	34.54	35.09	6.7	1.44
[73]	7	LiBr	Counter-flow	39.73	25.97	40.84	20.3	71.26	10.59	7.61	23.86	9.07
[76]	38	LiCl	Cross-flow	32.35	58.51	38.21	76.86	75.87	13.95	8.42	12.61	5.91
Total MARD				39.92	66.31	55.28	102.7	70.86	15.88	26.44	20.6	7.2

*Number of experimental points; ** How to read this Table: 34.77% is the MARD of the correlation taken from Ref. [25] with experimental data taken from Ref. [9].

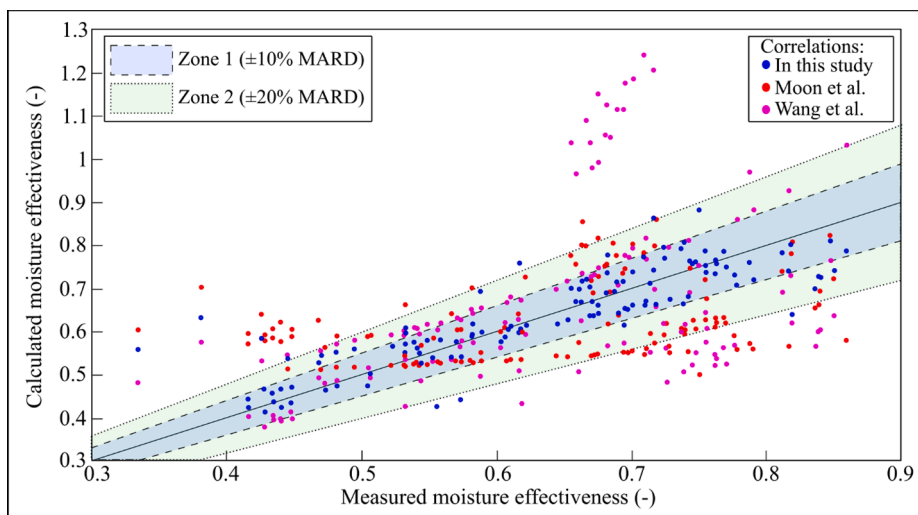


Fig. 16. Comparison of the predictive performance of new correlation with best performing correlations for moisture effectiveness of the dehumidification process.

Table 13
Performance of correlations for enthalpy effectiveness of the dehumidification process.

Ref.	N*	Liquid desiccant	Flow pattern	MARD (%) of different correlations			In this study
				taken from			
				[27]	[32]	[33]	
[9]	16	LiCl	Counter-flow	48.82**	74.87	84.93	5.72
[33]	14	LiCl	Counter-flow	22.58	91.04	4.11	4.06
[11]	15	LiCl	Cross-flow	4.8	82.2	13.7	6.52
[72]	23	LiCl	Counter-flow	57.37	91.33	23.8	10.6
[31]	5	LiCl	Cross-flow	15.27	89.14	8.1	9.9
[31]	5	LiBr	Cross-flow	46.07	86.06	5.54	4.09
[73]	7	LiBr	Counter-flow	28.13	88.62	26.47	9.9
[76]	38	LiCl	Cross-flow	27.03	88.83	24.94	3.86
Total MARD				32.68	86.81	27.4	6.4

*Number of experimental points; ** How to read this Table: 48.82% is the MARD of the correlation taken from Ref. [27] with experimental data taken from [9].

the regeneration process compared to the experimental values in most cases.

For the enthalpy effectiveness of the regeneration process, only Martin et al.'s correlation [27] was available for comparison, as illustrated in Table 15. As previously discussed in Sections 1 and 4.1, the above-mentioned correlation was developed for counter-flow patterns

and showed limited accuracy for experimental points obtained with cross-flow patterns.

5.3. Limitations of the study and future recommendations

This research is the first attempt to develop new correlations for the

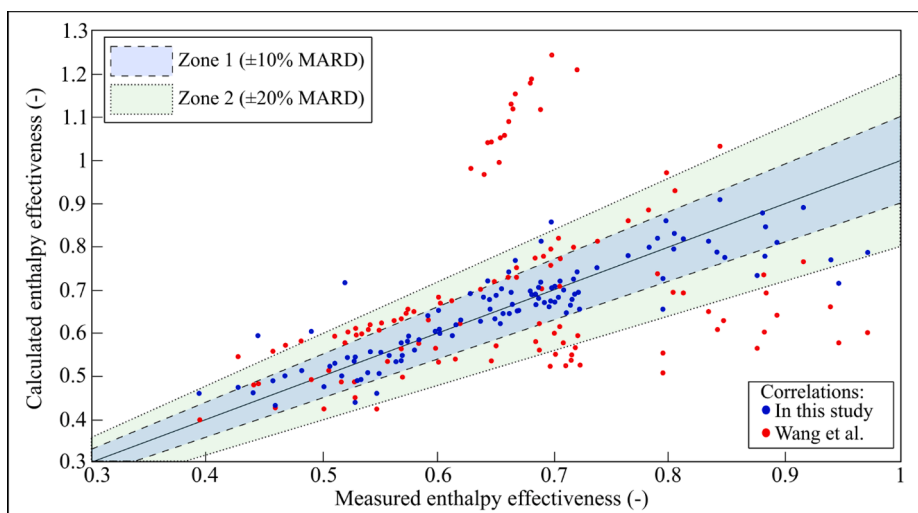


Fig. 17. Comparison of the predictive performance of new correlation with best performing correlation for enthalpy effectiveness of the dehumidification process.

Table 14
Performance of correlations for moisture effectiveness of the regeneration process.

Ref.	N*	Liquid desiccant	Flow pattern	MARD (%) of different correlations			In this study
				taken from [27]	[35]	[36]	
[31]	5	LiCl	Cross-flow	285.98**	154.49	49.08	21.25
[31]	5	LiBr	Cross-flow	214.3	26.07	11.79	16.46
[73]	4	LiBr	Counter-flow	5.52	87.09	35.72	2.66
[76]	38	LiCl	Cross-flow	374.67	119.68	40.23	3.4
Total MARD				322.32	111.52	38	6.31

*Number of experimental points; ** How to read this Table: 285.98% is the MARD of the correlation taken from Ref. [27] with experimental data taken from Ref. [31].

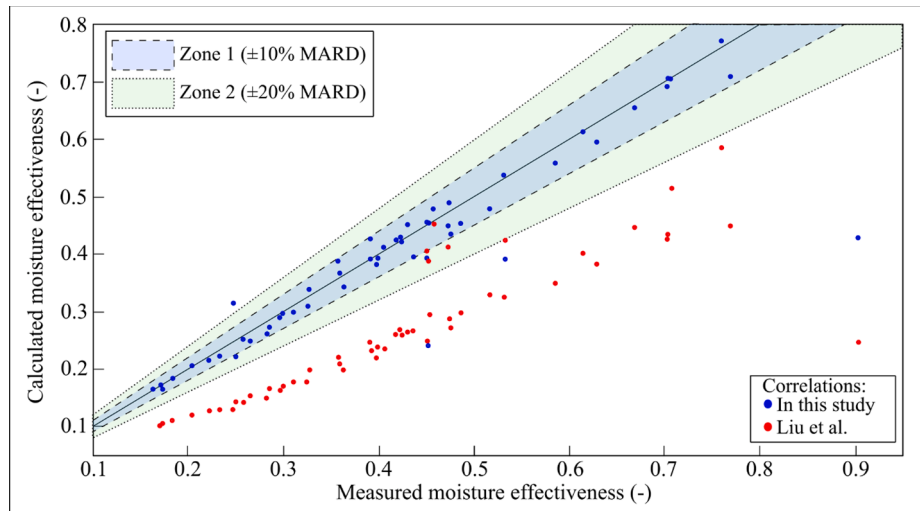


Fig. 18. Comparison of the predictive performance of new correlation with best performing correlation for moisture effectiveness of the regeneration process.

Table 15
Performance of correlations for enthalpy effectiveness of the regeneration process.

Ref.	N*	Liquid desiccant	Flow pattern	MARD (%) of different correlations	
				taken from [27]	In this study
[31]	5	LiCl	Cross-flow	108.37**	17.23
[31]	5	LiBr	Cross-flow	96.69	11.36
[73]	4	LiBr	Counter-flow	19.38	2.67
[76]	38	LiCl	Cross-flow	134.42	1.95
Total MARD				119.44	4.37

*Number of experimental points; ** How to read this Table: 108.37% is the MARD of the correlations taken from Ref. [27] with experimental data taken from Ref. [31].

dehumidification and regeneration process of liquid desiccants based on the use of secondary data (i.e. existing experimental data) and consider parameters previously neglected by literature (such as the contact time, hold-up based wetting and effective interfacial area). Although the accuracy of the newly developed correlations was demonstrated, the production of primary experimental data and their inclusion in the developed correlations would significantly increase the robustness of the research.

In the current study, the dataset used was limited to those with solution-to-air flow ratios of 0.5 and higher. By collecting more primary and secondary data in various operating ranges (including a relevant number of experimental data in the low-flow operating zone), the accuracy of the correlations could be further enhanced and its applicability extended. Future research should also focus on extending the

applicability of the developed correlations by including a larger number of types of packing materials and desiccant solutions. Whilst the correlations were developed considering a cellulose structured packing material, such as CELdek® 5090 and 7090, the research inspired the application of the correlations to packing materials different from cellulose. This could be realised by estimating the liquid hold-up through drainage volumetric test and determining the coefficients used in the Suess-Spiegel model [59].

6. Conclusion

New correlations were developed for quick performance estimation of both the dehumidification and the regeneration process of liquid desiccant systems. After analysis of previous correlations, identification of the main parameters, data collection, identification of the parameters affecting the performance of the heat and mass transfer and statistical analysis, these correlations were derived using 124 and 52 experimental points available from the literature ($m_{sol}/m_a > 0.5$) for the dehumidification and the regeneration process, respectively, and the following results were obtained for their predictive ability:

- For the dehumidification process, about 95% of the calculations for both moisture and enthalpy effectiveness had an error lower than $\pm 20\%$ with an average error of 7.2% and 6.4% for moisture and enthalpy effectiveness, respectively.
- For the regeneration process, about 92% and 94% of the calculations for moisture and enthalpy effectiveness had an error lower than $\pm 20\%$, respectively. The average error for the moisture effectiveness is 6.31% while that of the enthalpy effectiveness is 4.37%.

The newly developed correlations were also found to have a higher predictive ability than others in the literature. These newly developed correlations will be useful for designing and calculating the performance of liquid desiccant systems, as well as determining cost-effective solutions for the technology.

CRedit authorship contribution statement

Alessandro Giampieri: Conceptualization, Methodology, Software, Investigation, Writing – original draft. **Zhiwei Ma:** Conceptualization, Methodology, Writing – review & editing, Supervision. **Janie Ling-Chin:** Methodology, Visualization, Writing – review & editing, Supervision. **Huashan Bao:** Conceptualization, Methodology, Visualization. **Andrew J. Smallbone:** Supervision, Project administration, Funding acquisition. **Anthony Paul Roskilly:** Supervision, Project administration.

Declaration of Competing Interest

The authors declare that they have no known competing financial interests or personal relationships that could have appeared to influence the work reported in this paper.

Acknowledgments

The authors gratefully acknowledge the support from the Engineering and Physical Sciences Research Council for the Thermal Energy Challenge Network (EPSRC: EP/P005667/2), Industrial CASE (EPSRC: EP/N509292/1), DELTA PHI (EPSRC: EP/T022981/1) and Nissan Motor Manufacturing UK (Reference: 1823413), and the H-DisNet project funded by European Union's Horizon 2020 Research and Innovation Programme (Grant Agreement: 695780).

Appendix A. Supplementary material

Supplementary data to this article can be found online at <https://doi.org/10.1016/j.apenergy.2022.118962>.

References

- Mei L, Dai YJ. A technical review on use of liquid-desiccant dehumidification for air-conditioning application. *Renew Sustain Energy Rev* 2008;12(3):662–89.
- Daou K, Wang R, Xia Z. Desiccant cooling air conditioning: a review. *Renew Sustain Energy Rev* 2006;10(2):55–77.
- Mohammad AT, Mat SB, Sulaiman MY, Sopian K, Al-abidi AA. Historical review of liquid desiccant evaporation cooling technology. *Energy Build* 2013;67:22–33.
- Giampieri A, Ma Z, Smallbone A, Roskilly AP. Thermodynamics and economics of liquid desiccants for heating, ventilation and air-conditioning – An overview. *Appl Energy* 2018;220:455–79.
- Liu X-H, Jiang Yi, Qu K-Y. Analytical solution of combined heat and mass transfer performance in a cross-flow packed bed liquid desiccant air dehumidifier. *Int J Heat Mass Transf* 2008;51(17-18):4563–72.
- Ullah MR, Kettleborough CF, Gandhidasan P. Effectiveness of moisture removal for an adiabatic counterflow packed tower absorber operating with CaCl₂-air contact system. *J Sol Energy Eng* 1988;110(2):98–101.
- Gandhidasan P, Kettleborough CF, Ullah MR. Calculation of heat and mass transfer coefficients in a packed tower operating with a desiccant-air contact system. *J Sol Energy Eng* 1986;108(2):123–8.
- Onda K, Takeuchi H, Okumoto Y. Mass transfer coefficients between gas and liquid phases in packed columns. *J Chem Eng Jpn* 1968;1(1):56–62.
- Chung T-W, Ghosh TK, Hines AL. Comparison between random and structured packings for dehumidification of air by lithium chloride solutions in a packed column and their heat and mass transfer correlations. *Ind Eng Chem Res* 1996;35(1):192–8.
- Liu XH, Jiang Y, Qu KY. Heat and mass transfer model of cross flow liquid desiccant air dehumidifier/regenerator. *Energy Convers Manage* 2007;48(2):546–54.
- Chen Y, Zhang X, Yin Y. Experimental and theoretical analysis of liquid desiccant dehumidification process based on an advanced hybrid air-conditioning system. *Appl Therm Eng* 2016;98:387–99.
- Yin Y, Qian J, Zhang X. Recent advancements in liquid desiccant dehumidification technology. *Renew Sustain Energy Rev* 2014;31:38–52.
- Luo Y, Yang H, Lu L, Qi R. A review of the mathematical models for predicting the heat and mass transfer process in the liquid desiccant dehumidifier. *Renew Sustain Energy Rev* 2014;31:587–99.
- Dai YJ, Zhang HF. Numerical simulation and theoretical analysis of heat and mass transfer in a cross flow liquid desiccant air dehumidifier packed with honeycomb paper. *Energy Convers Manage* 2004;45(9-10):1343–56.
- Li X, Liu S, Tan KK, Wang Q-G, Cai W-J, Xie L. Dynamic modeling of a liquid desiccant dehumidifier. *Appl Energy* 2016;180:435–45.
- Wang L, Xiao Fu, Niu X, Gao D-c. A dynamic dehumidifier model for simulations and control of liquid desiccant hybrid air conditioning systems. *Energy Build* 2017; 140:418–29.
- Sadasivam M, Balakrishnan AR. Effectiveness-NTU method for design of packed bed liquid desiccant dehumidifiers. *Chem Eng Res Des* 1992;70(A6):572–7.
- Ren C-Q. Corrections to the simple effectiveness-NTU method for counterflow cooling towers and packed bed liquid desiccant-air contact systems. *Int J Heat Mass Transf* 2008;51(1-2):237–45.
- Liu XH, Jiang Y. Coupled heat and mass transfer characteristic in packed bed dehumidifier/regenerator using liquid desiccant. *Energy Convers Manage* 2008;49(6):1357–66.
- Liu XH, Qu KY, Jiang Y. Empirical correlations to predict the performance of the dehumidifier using liquid desiccant in heat and mass transfer. *Renew Energy* 2006; 31(10):1627–39.
- Kim M-H, Park J-Y, Jeong J-W. Simplified model for packed-bed tower regenerator in a liquid desiccant system. *Appl Therm Eng* 2015;89:717–26.
- Zendehboudi A, Tatar A, Li X. A comparative study and prediction of the liquid desiccant dehumidifiers using intelligent models. *Renew Energy* 2017;114: 1023–35.
- Crofoot L. Experimental evaluation and modeling of a solar liquid desiccant air conditioner; 2012.
- Wen T, Lu L. A review of correlations and enhancement approaches for heat and mass transfer in liquid desiccant dehumidification system. *Appl Energy* 2019;239: 757–84.
- Chung T-W. Predictions of moisture removal efficiencies for packed-bed dehumidification systems. *Gas Sep Purif* 1994;8(4):265–8.
- Chung T-W, Luo C-M. Vapor pressures of the aqueous desiccants. *J Chem Eng Data* 1999;44(5):1024–7.
- Martin V, Goswami DY. Effectiveness of heat and mass transfer processes in a packed bed liquid desiccant dehumidifier/regenerator. *HVAC&R Res* 2000;6(1): 21–39.
- Abdul-Wahab SA, Zurigat YH, Abu-Arabi MK. Predictions of moisture removal rate and dehumidification effectiveness for structured liquid desiccant air dehumidifier. *Energy* 2004;29(1):19–34.
- Liu XH, Zhang Y, Qu KY, Jiang Y. Experimental study on mass transfer performances of cross flow dehumidifier using liquid desiccant. *Energy Convers Manage* 2006;47(15-16):2682–92.
- Moon CG, Bansal PK, Jain S. New mass transfer performance data of a cross-flow liquid desiccant dehumidification system. *Int J Refrig* 2009;32(3):524–33.
- Liu XH, Yi XQ, Jiang Y. Mass transfer performance comparison of two commonly used liquid desiccants: LiBr and LiCl aqueous solutions. *Energy Convers Manage* 2011;52(1):180–90.
- Gao WZ, Liu JH, Cheng YP, Zhang XL. Experimental investigation on the heat and mass transfer between air and liquid desiccant in a cross-flow dehumidifier. *Renew Energy* 2012;37(1):117–23.
- Wang L, Xiao Fu, Zhang X, Kumar R. An experimental study on the dehumidification performance of a counter flow liquid desiccant dehumidifier. *Int J Refrig* 2016;70:289–301.
- Fumo N, Goswami DY. Study of an aqueous lithium chloride desiccant system: air dehumidification and desiccant regeneration. *Sol Energy* 2002;72(4):351–61.
- Sultan GI, Hamed AM, Sultan AA. The effect of inlet parameters on the performance of packed tower-regenerator. *Renew Energy* 2002;26(2):271–83.
- Liu XH, Jiang Y, Chang XM, Yi XQ. Experimental investigation of the heat and mass transfer between air and liquid desiccant in a cross-flow regenerator. *Renew Energy* 2007;32(10):1623–36.
- Geyer P, Buchholz M, Buchholz R, Provost M. Hybrid thermo-chemical district networks—Principles and technology. *Appl Energy* 2017;186:480–91.
- Geyer P, Delwati M, Buchholz M, Giampieri A, Smallbone A, Roskilly AP, et al. Use cases with economics and simulation for thermo-chemical district networks. *Sustainability* 2018;10(3):599. <https://doi.org/10.3390/su10030599>.
- Giampieri A, Ma Z, Smallbone A, Roskilly AP. Thermodynamics and economics of liquid desiccants for heating, ventilation and air-conditioning—an overview. *Appl Energy* 2018;220:455–79.
- Giampieri A, Ma Z, Ling Chin J, Smallbone A, Lyons P, Khan I, et al. Techno-economic analysis of the thermal energy saving options for high-voltage direct current interconnectors. *Appl Energy* 2019;247:60–77.
- Cho H-J, Cheon S-Y, Jeong J-W. Experimental analysis of dehumidification performance of counter and cross-flow liquid desiccant dehumidifiers. *Appl Therm Eng* 2019;150:210–23.
- Anderson D, Burnham K. Model selection and multi-model inference, Second. NY: Springer-Verlag; 2004. 63(2020): p. 10.
- Motulsky H, Christopoulos A. Fitting models to biological data using linear and nonlinear regression: a practical guide to curve fitting. Oxford University Press; 2004.
- Conde MR. Properties of aqueous solutions of lithium and calcium chlorides: formulations for use in air conditioning equipment design. *Int J Therm Sci* 2004;43(4):367–82.
- Elsarrag E, Ali EE, Jain S. Design guidelines and performance study on a structured packed liquid desiccant air-conditioning system. *HVAC&R Res* 2005;11(2):319–37.

- [46] Ling-Chin J, et al. State-of-the-Art Technologies on Low-Grade Heat Recovery and Utilization in Industry. *Energy Conversion: Current Technologies and Future Trends*, 2019: p. 55.
- [47] Potnis SV, Lenz TG. Dimensionless mass-transfer correlations for packed-bed liquid-desiccant contactors. *Ind Eng Chem Res* 1996;35(11):4185–93.
- [48] Laknizi A, et al. Performance analysis and optimal parameters of a direct evaporative pad cooling system under the climate conditions of Morocco. *Case Stud Therm Eng* 2019;13:100362.
- [49] Tsai RE. *Mass transfer area of structured packing*; 2010.
- [50] Zhang Li, Hihara E, Matsuoka F, Dang C. Experimental analysis of mass transfer in adiabatic structured packing dehumidifier/regenerator with liquid desiccant. *Int J Heat Mass Transf* 2010;53(13-14):2856–63.
- [51] Olujić Z, Kamerbeek AB, de Graauw J. A corrugation geometry based model for efficiency of structured distillation packing. *Chem Eng Process Process Intensif* 1999;38(4-6):683–95.
- [52] Kolev N. *Packed bed columns: for absorption, desorption, rectification and direct heat transfer*. Elsevier; 2006.
- [53] Bravo JL, Rocha JA, Fair JR. Pressure drop in structured packings. *Hydrocarbon Process; (United States)* 1986;65(3).
- [54] Stichlmair J, Bravo JL, Fair JR. General model for prediction of pressure drop and capacity of countercurrent gas/liquid packed columns. *Gas Sep Purif* 1989;3(1): 19–28.
- [55] Rocha JA, Bravo JL, Fair JR. Distillation columns containing structured packings: a comprehensive model for their performance. 1. Hydraulic models. *Ind Eng Chem Res* 1993;32(4):641–51.
- [56] Al-Farayedhi AA, Gandhidasan P, Al-Mutairi MA. Evaluation of heat and mass transfer coefficients in a gauze-type structured packing air dehumidifier operating with liquid desiccant. *Int J Refrig* 2002;25(3):330–9.
- [57] Ertas A, Anderson EE, Kavasogullari S. Comparison of mass and heat transfer coefficients of liquid-desiccant mixtures in a packed column. *J Energy Res Technol* 1991;113(1):1–6.
- [58] Kabeel AE, Khalil A, Elsayed SS, Alatyar AM. Dynamic behaviour simulation of a liquid desiccant dehumidification system. *Energy* 2018;144:456–71.
- [59] Suess P, Spiegel L. Hold-up of Mellapak structured packings. *Chem Eng Process Process Intensif* 1992;31(2):119–24.
- [60] Stockfleth R, Brunner G. Holdup, pressure drop, and flooding in packed countercurrent columns for the gas extraction. *Ind Eng Chem Res* 2001;40(1): 347–56.
- [61] Liu X, Liu X, Zhang T, Xie Y. Experimental analysis and performance optimization of a counter-flow enthalpy recovery device using liquid desiccant. *Build Serv Eng Res Technol* 2018;39(6):679–97.
- [62] Erasmus AB. *Mass transfer in structured packing*. Stellenbosch: University of Stellenbosch; 2004.
- [63] Rahimi A, Babakhani D. Mathematical modeling of a packed-bed air dehumidifier: The impact of empirical correlations. *J Petrol Sci Eng* 2013;108:222–9.
- [64] Shi MG. Effective interfacial area in packed columns. *German Chem Eng* 1985;8: 87–96.
- [65] de Brito MH, von Stockar U, Bangerter AM, Bomio P, Laso M. Effective mass-transfer area in a pilot plant column equipped with structured packings and with ceramic rings. *Ind Eng Chem Res* 1994;33(3):647–56.
- [66] Rocha JA, Bravo JL, Fair JR. Distillation columns containing structured packings: a comprehensive model for their performance. 2. Mass-transfer model. *Ind Eng Chem Res* 1996;35(5):1660–7.
- [67] Brunazzi E, et al. Interfacial area of mellapak packing: Absorption of 1, 1, 1-trichloroethane by Genosorb 300. *Chem Eng Technol: Ind Chem-Plant Equipment-Process Eng-Biotechnol* 1995;18(4):248–55.
- [68] Brunazzin E, Paglianti A. Mechanistic pressure drop model for columns containing structured packings. *AIChE J* 1997;43(2):317–27.
- [69] Dong C, Qi R, Lu L, Wang Y, Wang L. Comparative performance study on liquid desiccant dehumidification with different packing types for built environment. *Sci Technol Built Environ* 2017;23(1):116–26.
- [70] Lychnos G, Davies PA. A solar powered liquid-desiccant cooling system for greenhouses. *Acta Horti* 2008;(797):95–109. <https://doi.org/10.17660/ActaHortic.2008.797.11>.
- [71] Bassuoni MM. An experimental study of structured packing dehumidifier/regenerator operating with liquid desiccant. *Energy* 2011;36(5):2628–38.
- [72] Tang C, Vafai K, Zhang D. Mass transfer performance of the LiCl solution dehumidification process. *Int Commun Heat Mass Transfer* 2017;85:139–46.
- [73] Xie Y, Zhang T, Liu X. Performance investigation of a counter-flow heat pump driven liquid desiccant dehumidification system. *Energy* 2016;115:446–57.
- [74] Mohamed ASA, Ahmed MS, Hassan AAM, Hassan MS. Performance evaluation of gauze packing for liquid desiccant dehumidification system. *Case Stud Therm Eng* 2016;8:260–76.
- [75] Wang X, Cai W, Lu J, Sun Y, Ding X. Heat and mass transfer model for desiccant solution regeneration process in liquid desiccant dehumidification system. *Ind Eng Chem Res* 2014;53(7):2820–9.
- [76] Varela RJ, Yamaguchi S, Giannetti N, Saito K, Harada M, Miyauchi H. General correlations for the heat and mass transfer coefficients in an air-solution contactor of a liquid desiccant system and an experimental case application. *Int J Heat Mass Transf* 2018;120:851–60.
- [77] Lazzarin R, Nalini L. *Air Humidification: Technical, Health and Energy Aspects*. Carel SpA; 2004.
- [78] Pátek J, Klomfar J. A computationally effective formulation of the thermodynamic properties of LiBr–H₂O solutions from 273 to 500 K over full composition range. *Int J Refrig* 2006;29(4):566–78.
- [79] Factor HM, Grossman G. A packed bed dehumidifier/regenerator for solar air conditioning with liquid desiccants. *Sol Energy* 1980;24(6):541–50.
- [80] Seber GA. Nonlinear regression models. In: *The linear model and hypothesis*. Springer; 2015. p. 117–28.